Semester Project

Economic and Environmental Assessment of Heat Prosumer Communities

Autumn Term 2023

Supervised by:
Prof. Dr. Gabriela Hug
Dr. Hanmin Cai
Dr. Binod Prasad Koirala
Prof. Dr. Philipp Schütz

Author:
Bernadino, Bernadino

Declaration of Originality

I hereby declare that the written work I have submitted entitled

Economic and Environmental Assessment of Heat Prosumer Communities

is original work which I alone have authored and which is written in my own words.[1]

Author(s)

Bernadino	Bernadino

Student supervisor(s)

Hanmin	Cai
Binod Prasad	Koirala
Philipp	Schütz

Supervising lecturer

Gabriela	Hug

With the signature, I declare that I have been informed regarding normal academic citation rules and that I have read and understood the information on 'Citation etiquette' (https://www.ethz.ch/content/dam/ethz/main/education/rechtliches-abschluesse/leistungskontrollen/plagiarism-citationetiquette.pdf). The citation conventions usual to the discipline in question here have been respected.

The above written work may be tested electronically for plagiarism.

Zürich, 01/02/2024

Place and date

Signature

[1]Co-authored work: The signatures of all authors are required. Each signature attests to the originality of the entire piece of written work in its final form.

Contents

Abstract

Swiss energy landscape is shifting to incorporate more renewable energy technologies to meet its 2050 net-zero goals. These technologies also facilitate the transition of households from passive consumers to active prosumers in the form of energy community. With the possibilities of decentralised energy generation, connections between houses to exchange energy become more apparent. One example of such collective is a heat prosumer community that trade, produce, and store thermal energy. Despite the newfound technological benefits of energy community, few studies have been made to investigate its viability through economic and environmental lenses. This study proposes a framework to assess a heat prosumer community under these metrics. An energy hub model with multi-energy, multi-hub, and multi-objective optimisation capabilities are formulated. The model is then implemented in a case study involving three thermally connected buildings in Basel under the nanoverbund project. The results from this case study are used to provide three preliminary findings. First, economic and environmental viability of such a community is strongly dependent on how much loss the thermal network has. Second, the network is made redundant when all houses are given the same opportunities to decarbonise at the same time. Third, cheap wood is a promising alternative to the use of the network, by providing a cheap, clean energy source for each house in the community.

Symbols

Symbols

$f_{cost}(x)$	total cost function
$f_{CO2}(x)$	total carbon emission function
E_{elec}	electric energy
$E_{Q,HT}$	high temperature heat energy
$E_{Q,LT}$	low temperature heat energy
E^d	energy demand
E^d_{elec}	electricity demand
E^d_{DHW}	domestic hot water demand
E^d_{SH}	space heating demand
E^s	energy supply
E^{import}	energy imported to the community
$E^{availability}$	amount of energy available to be used
E^{in}	energy input to a conversion technology
E^{out}	energy output from a conversion technology
P^{conv}	operational load of a conversion technology
$P^{conv,cap}$	capacity load of a conversion technology
E^{stor}	operational energy stored at a storage technology
$E^{stor,cap}$	capacity energy stored at a storage technology
Q^{ch}	charging energy flow at a storage technology
Q^{disch}	discharging energy flow at a storage technology
L_{ab}	operational network flow through a link from hub a to hub b
L^{cap}_{ab}	capacity network flow through a link from hub a to hub b
ℓ^{stor}	standing loss of a storage technology
$\ell^{network}$	network loss of a link per length of the link
η_H	high temperature efficiency of heat converter device
η_L	low temperature efficiency of heat converter device
$\eta_{VN,H}$	efficiency of virtual conversion node to supply DHW
$\eta_{VN,L}$	efficiency of virtual conversion node to supply SH
η^{ch}	efficiency of charging of a storage technology
η^{disch}	efficiency of discharging of a storage technology
N^{EC}	set of energy carriers
N^{conv}	set of conversion technologies
N^{stor}	set of storage technologies
N^{hub}	set of hubs

N^{TS}	number of time steps in the time horizon
$N^{bld,el}$	number of building elements
x	decision variables of the optimisation problem
y_{ab}	length of a link from hub a to hub b
t	one time step evaluated
c^{CAPEX}	capital expenditures of a technology per capacity
c^{OPEX}	operating expenditures of a technology per capacity
$c^{O\&M,var}$	variable operational and maintenance costs per output energy
c^{import}	price of energy imported
e^{import}	carbon emission of energy imported
c_p	specific heat capacity
C_p	heat capacity
ρ	mass density
ΔT	temperature difference
V^{stor}	capacity volume of a storage technology
A^{ref}	reference area of a building element

Acronyms and Abbreviations

GHG	Green House Gas
ZEV	Zusammenschluss zum Eigenverbrauch
PV	Photovoltaic
SIA	The Swiss Society of Engineers and Architects
BEM	Building Energy Modelling
TRNSYS	Transient System Simulation
HVAC	Heating, ventilation, and air conditioning
IDA ICE	IDA Indoor Climate and Energy
CESAR	Combined Energy Simulation And Retrofitting
GIS	Geographic Information System
CAD	Computer-Aided Design
CEA	City Energy Analyst
IPCC	Intergovernmental Panel on Climate Change
MILP	Mixed-Integer Linear Programming
DES	Decentralised Energy System
UI	User Interface
GSHP	Ground Source Heat Pump
ASHP	Air Source Heat Pump
SH	Space Heating
SC	Space Cooling
Elec.	Electricity
DHW	Domestic Hot Water
GFA	Gross Floor Area
SoC	State of Charge
CAPEX	Capital Expenditure
OPEX	Operating Expenditure
O&M	Operation and Maintenance

Chapter 1

Introduction

1.1 Background

With the advent of energy transition policies and the increasing maturation of renewable energy technologies, a once traditionally perceived as a consumerist stakeholder in the energy system, the household, is presented with a new opportunity to play an active role in the future of energy dynamics. Typical residential units can now be transformed into renewable energy-based prosumer entities whereby energy is not only consumed, but also sustainably produced and possibly stored. In addition to reducing Green House Gas (GHG) emissions, prosumption is shown to benefit the energy system by enhancing its robustness through decentralisation and demand flexibility [1]. In some cases [2], [3], [4], these individual prosumer entities collaborated and formed collective energy communities. In the European Union, these communities are legally defined through two directives: Directive (EU) 2019/944 for citizen energy communities and Directive (EU) 2018/2001 for renewable energy communities [5]. Through these directives, an energy community is a commonly and legally accepted entity in the region that enables citizens and local stakeholders to produce, manage, and consume their own energy.

As part of the energy strategy 2050 enforcement [6], Swiss energy system is expected to take measures to increase the use of renewable energy sources. This push towards renewable energy and the implementation of an energy community are prevalent in the electricity sector through the self-consumption association called *Zusammenschluss zum Eigenverbrauch* (ZEV) [7]. However, the same initiative is yet to be seen in the heating energy sector. Current statistic shows that around two-thirds of Swiss households are still heated by oil and natural gas as of 2022 [8]. Coupled this fact with the recent Europe's energy crisis [9] and the 70-percent dependency of Swiss energy supply on imports from neighbouring European countries [10], additional actions are needed to achieve the energy transition goals and improve the resilience of the energy system. One possible answer to this problem is to introduce more decentralised, interconnected prosumer communities in Swiss heating energy landscape.

Despite the apparent technological benefits, the economic and environmental viabilities of such collective prosumer concept have not been comprehensively considered. With the possibility of significant upfront cost in switching to renewable technologies, potential prosumer households expect incentives such as a good return on investment when participating in such a project [11]. Connecting houses in a community with heating networks also introduces new technical metrics, such as thermal network losses, that need to be considered. These metrics may influence the environmental soundness of introducing a new renewable technology in the neighbourhood. Weighing in these challenges and benefits, more systematic economic and environmental assessments of a prosumer community are needed to justify its feasibility.

1.2 Contribution and Overview

This study contributes uniquely in the following ways:

1. Proposing an initial framework and model for assessing economic and environmental impacts of a decentralised, residential heat prosumer community in Switzerland. This framework includes an extensive review on tools required for evaluating an energy system, a multi-objective optimisation problem formulation for that system, an implementation procedure to solve the problem in a scenario-based case study setting.

2. Providing preliminary findings on the impacts and trade-offs of different technology mixes implemented in the community using a case study involving three thermally interconnected buildings. The findings answered the following questions:

    - How does thermal network loss impact the deployment of that system in a heat prosumer community?
    - What are the technologies installed if all hubs in the community were given the same technology candidates to decarbonise?
    - With increasing popularity of wood boilers, does it still make sense to use them in the community if prices were to rise in the future?

This report is organised as such: in Chapter 2, an assessment framework and ehubX modelling and formulation are detailed; in Chapter 3, case study conditions, data inputs, and scenarios assessed are introduced; in Chapter 4, the optimisation results of the case study are presented; and lastly in Chapter 5, the study is concluded, and future works are discussed. Appendices A and B are included to show the comprehensive literature review and critical tool comparison done for this study.

Chapter 2

Methodology

2.1 Workflow

To evaluate a heat prosumer community economically and environmentally, a three-step process is devised, as summarised in Figure 2.1. First, an optimisation problem is formulated and modelled to find optimum solutions between cost and emission. The formulation is not only solving supply-conversion-demand balance within a single hub, but it also includes a network problem spanning throughout the neighbourhood. This step is detailed in this methodology chapter.

For the next two steps, a case study is selected. In the second step, preparation of necessary input data is made. The minimum inputs required are demand profiles, prices, and emissions data for different type of energy carriers and technologies, and renewable potentials, which for this study consist of solar irradiation. Lastly, the problem is solved under different input conditions to evaluate the soundness of heat prosumer concept implementation. These steps are detailed in Chapter 3.

2.2 ehubX Model

2.2.1 General Overview

The interconnectedness between different supplies, technologies, demands, and inter-hub networks are modelled in ehubX and depicted in Figure 2.2. The schema here

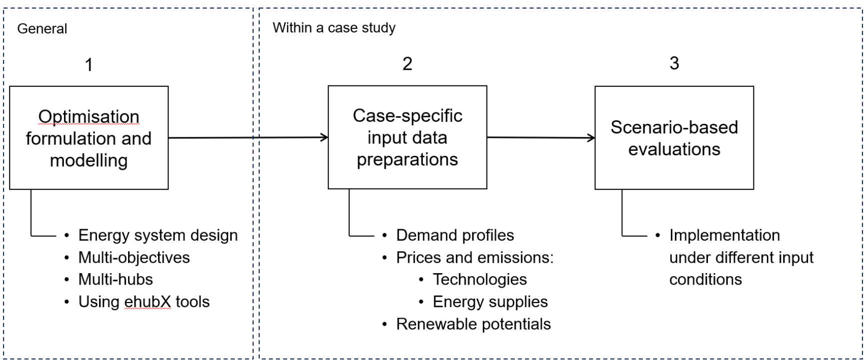

Figure 2.1: Workflow for economic and environmental assessment of a heat prosumer community.

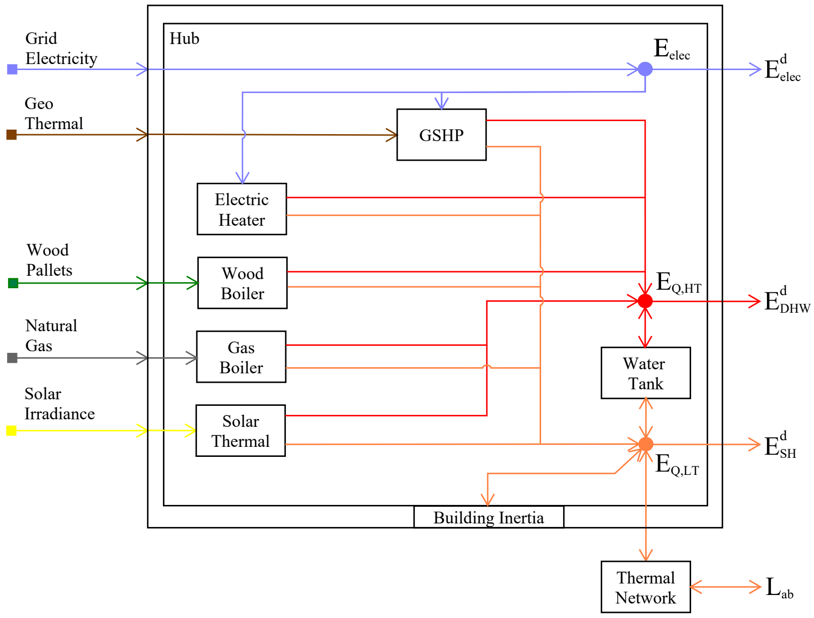

Figure 2.2: Schema of general ehubX implementation

represents the complete technology mixes explored in this study. Since the main focus of this study is heat prosumer communities, some simplifications to the hub are made, such as no cooling demand is considered and electricity demand is purely fulfilled through grid electricity. Increasing the complexity of supplies, technologies, and demands is a possible extension to this initial framework.

Most energy flows work in a feed forward manner. Storage technologies and networks work reversibly. For heating devices, supplying different temperatures may result in different efficiency levels. In the community with small houses, it is not realistic to allow the optimisation to arrive with multiple technologies of the same kind. To accommodate the phenomenon and not violate the constraint, virtual nodes and intermediary thermal energies are created. Figure 2.3 displays such a modelling concept. A heat conversion device is modelled with low temperature efficiency η_L and output of virtual intermediary thermal energy. This intermediary energy is used by two virtual conversion nodes: for low temperature space heating, and high temperature DHW. The low temperature virtual node has injective efficiency $\eta_{VN,L}$, while the high one has efficiency $\eta_{VN,H}$ equals to the ratio of the heat device high temperature efficiency η_H over its lower one η_L.

Multi-objective optimisation is set in ehubX and solved using Gurobi solver [12]. The two objectives are cost and carbon emission, with the first objective being cost. Number of Pareto points is set at 4. ehubX modules used in this study are network module, storage module, and solar area module, while other modules are set to be inactive.

2.2.2 Optimisation Formulation

The optimisation problem for this study is formulised in Equation 2.1. The objectives are to minimise cost and carbon emission, subject to several constraints:

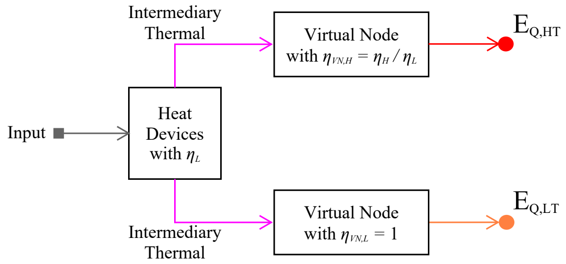

Figure 2.3: Schema of heat conversion device efficiencies

energy balance, energy import availability, conversion technology efficiency, conversion technology capacity, storage state-of-charge (SoC), storage technology capacity, and network flow capacity. A set of decision variables x includes five components: capacity of a conversion technology, $P^{conv,cap}$; capacity of a storage technology, $E^{stor,cap}$; capacity of a network technology, L^{cap}; energy output of a conversion technology, E^{out}; and energy imported to the community, E^{import}.

$$
\begin{array}{llll}
\min\limits_{x} & \multicolumn{3}{l}{(f_{cost}(x), f_{CO2}(x))} \\
 & \multicolumn{3}{l}{x \in \{P^{conv,cap}, E^{stor,cap}, L^{cap}, E^{out}, E^{import}\}} \\
\text{s.t.} & E^{d}_{j,a,t} = E^{s}_{j,a,t} & & \\
 & E^{import}_{j,a,t} \leq E^{availability}_{j,a,t} & & \forall j \in N^{EC} \\
 & E^{out}_{m,t} = \eta_m E^{in}_{m,t} & & \\
 & P^{conv}_{m,t} \leq P^{conv,cap}_{m} & & \forall m \in N^{conv} \\
 & E^{stor}_{n,t+1} = (1 - \ell^{stor}_{n}) E^{stor}_{n,t} + \eta^{ch}_{n} Q^{ch}_{n} - \dfrac{Q^{disch}_{n}}{\eta^{disch}_{n}} & & \\
 & E^{stor}_{n,t} \leq E^{stor,cap}_{n} & & \forall n \in N^{stor} \\
 & L_{ab,t} \leq L^{cap}_{ab} & & \forall a, b \in N^{hub}; a \neq b \\
 & & & \forall t \in N^{TS}
\end{array}
\tag{2.1}
$$

In Equation 2.2, the cost function is defined. The total cost consists of technology and energy import costs. Three components are defined for technology costs: capital or investment expenditures (CAPEX) and operating expenditures (OPEX), both depend on the capacity installed; and operational and maintenance (O&M) cost that depends on total energy outputted. These technology costs are applied to conversion, storage, and network technologies. Energy import costs are evaluated per time step, as the energy price may temporally vary.

In Equation 2.3, the emission function is defined. The total emission for this study is assumed to be only influenced by the energy imported. This energy emission is evaluated per time step, as the imported energy carbon intensity may temporally vary.

$$
\begin{aligned}
f_{cost}(x) = \sum_{m \in N^{conv}} & \left(E_m^{conv,cap} \left(c_m^{CAPEX} + c_m^{OPEX} \right) + \sum_{t=1}^{N^{TS}} \left(E_{m,t}^{out} c_{m,t}^{O\&M,var} \right) \right) \\
& + \sum_{n \in N^{stor}} \left(E_n^{stor,cap} \left(c_n^{CAPEX} + c_n^{OPEX} \right) \right) \\
& + \sum_{a \in N^{hub}} \sum_{b \in N^{hub}, b \neq a} \left(y_{ab} \left(c_{ab}^{CAPEX} + L_{ab}^{cap} c_{ab}^{OPEX} \right) \right) \\
& + \sum_{j \in N^{EC}} \sum_{t=1}^{N^{TS}} E_{j,t}^{import} c_{j,t}^{import}
\end{aligned} \tag{2.2}
$$

$$
f_{CO2}(x) = \sum_{j \in N^{EC}} \sum_{t=1}^{N^{TS}} E_{j,t}^{import} e_{j,t}^{import} \tag{2.3}
$$

The energy j supplied in time step t and hub a used for energy balance constraint is further elaborated in Equation 2.4. Four general sources of energy are considered in this implementation: energy directly imported from outside neighbourhood sources, energy output from conversion technologies, energy drawn from storage technologies, and energy locally traded from other hubs in the prosumer community. The energy imported E^{import} is a subset of all energy carriers in the formulation that is readily available to be used for the corresponding demands. One example for this study is electricity grid, which can be directly imported and used.

$$
\begin{aligned}
E_{j,a,t}^{s} = E_{j,a,t}^{import} + \sum_{m \in N^{conv}} E_{m,a,t}^{out} + \sum_{n \in N^{stor}} \left(\frac{Q_{n,a,t}^{disch}}{\eta_n^{disch}} - \eta_n^{ch} Q_{n,a,t}^{ch} \right) \\
+ \sum_{b, b \neq a}^{N^{hub}} \left(\left(1 - \ell_{ab}^{network} y_{ab} \right) \left(L_{ab} - L_{ba} \right) \right)
\end{aligned} \tag{2.4}
$$

Chapter 3

Case Study

3.1 Case Description

Three thermally connected single family houses in Basel City under the nanoverbund project are selected for the implementation of this study framework. The buildings are constructed in the 1930s and renovated in the 1990s, with gross floor area (GFA) ranging from 130m^2 to 200m^2. The energy systems for this community are shown in Figure 3.1. For this study, House 200, House 198, House 196 are respectively renamed as H1, H2, and H3. All houses are connected to the electrical grid. H1 has similar configurations with H3 with solar thermal collectors, domestic hot water tanks, and gas boilers. H2 is supplied with a GSHP with a thermal storage tank. The houses are connected with each other via water heat pipes. Roof areas available for solar generation are summarised in Table 3.1. Currently, H1 has installed 6m^2 on its flat roof, while H2 has installed 6m^2 on its west roof. Thermal pipe lengths between houses are approximated to be H1-H2 (L12) = 10m, H2-H3 (L23) = 12m, H1-H3 (L13) = 18m.

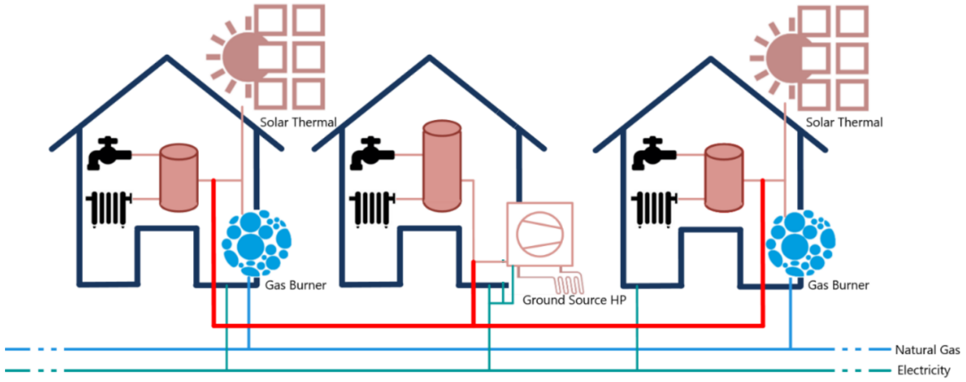

Figure 3.1: Nanoverbund energy systems

Table 3.1: Summary of available solar areas (m^2)

Orientation (Pitch)	H1	H2	H3
Flat Roof	6	0	0
North Roof (30°)	0	0	6
East Roof (30°)	20	28	10
South Roof (30°)	0	0	6
West Roof (30°)	3	18	25

3.2 Input Data

3.2.1 Time Horizon

In this study, the optimisation problem is modelled within a time horizon of one year. The temporal resolution for this study is set as hourly. The total number of time steps is, therefore, 8760 time steps.

3.2.2 Demand Data

In this study, BEM through CESAR is chosen to gather demand profiles of individual buildings in the community. This study uses demand profiles generated from previous study [13] on different typical houses in Northern Switzerland. Three single family houses with different features are selected for this study and summarises in Table 3.2. The demand profiles extracted are hourly demands of electricity, space heating, and DHW within a period of one year. Electricity demand is cleaned from energy demanded by the use of heat pumps or any other heat-providing electrical devices. This preprocessing ensures no demand is counted several times. The three house demands are approximated to H1, H2, and H3 from nanoverbund study case based on the GFA comparison. The profiles are shown in Figure 3.2.

Table 3.2: Summary of single family house features

	H1	H2	H3
Year of Construction	1968	1968	1982
Number of Storey	1	1	1
Floor Height	4.3	4.3	6.35
GFA (m^2)	95	106	181
Glazing Ratio	0.17	0.17	0.25

3.2.3 Energy Supply Data

There are five energy carriers selected as supply for this study: grid electricity, natural gas, geothermal, solar, and wood. Table 3.3 summarises the cost and emission data related to each energy supply which is extracted from [14]. Grid electricity cost and carbon intensity profiles are 2022 data gathered from [15]. Since the Swiss supply system is deemed to be sufficiently adequate in supplying three single family houses, most availability of the supplies are set to be infinite. For solar potential, a weather file is retrieved from [16] for Basel City, taken at St. Chrischona. From this weather file, direct normal radiation is gathered. This profile is then processed using methods described in [17] to get five solar irradiation profiles on different surfaces at nanoverbund houses.

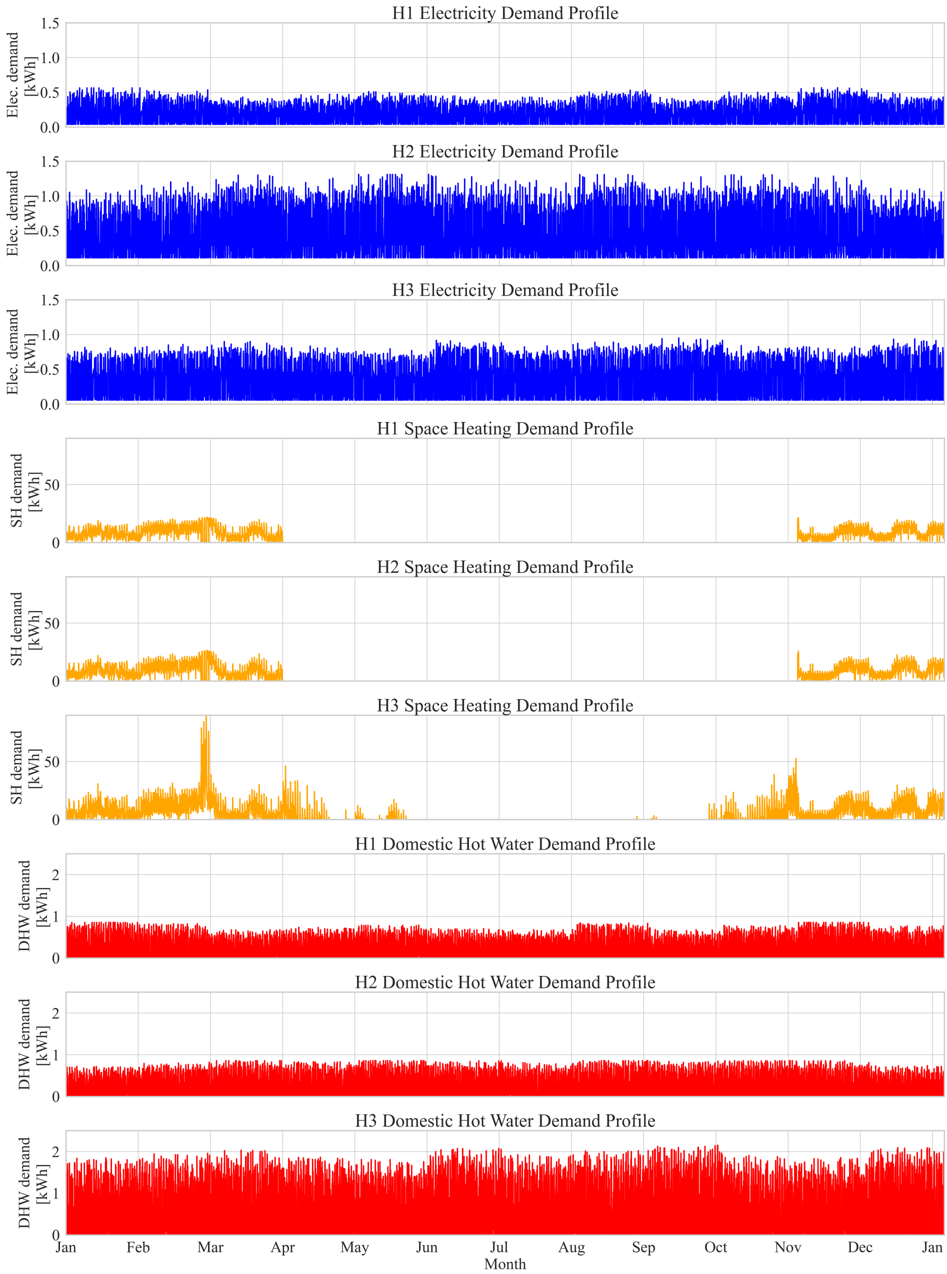

Figure 3.2: Demand profiles

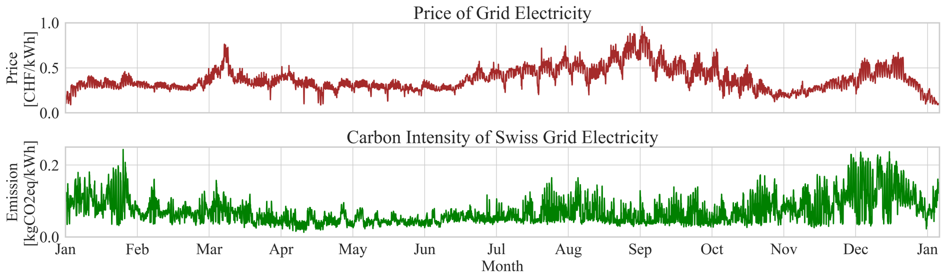

Figure 3.3: Grid electricity profiles

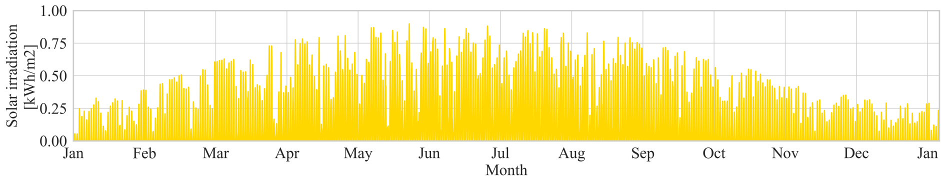

Figure 3.4: Normal solar irradiation for Basel

3.2.4 Technology Data

Three groups of technologies are considered in this study: conversion, storage, and network technologies. Table 3.4 summarises conversion technology data and Table 3.5 summarises storage technology data. The efficiencies, CAPEX, OPEX, and O&M variable costs are taken from [14] [18] [19]. As this study involves three small single family houses, embodied emission for all conversion technologies are ignored.

For storage technologies, maximum capacities,$E^{cap}_{stor,WT}$, are calculated to avoid overly sized tanks. DHW tanks that are linked to solar thermal collectors are assumed to have a maximum volume, $V_{stor,WT}$, of 100L, while thermal tanks that are linked to GSHP is capped at 500L. The temperature differences, ΔT, are assumed to be 50°C and 30°C respectively. The storage capacity is calculated using Equation 3.1 with water specific heat capacity, $c_{p,water}$, equals 4.18kJ/kg*K and water density, ρ_{water}, equals 1000kg/m^3.

$$E^{stor,cap}_{WT} = c_{p,water} \cdot \rho_{water} \cdot V^{stor}_{WT} \cdot \Delta T \tag{3.1}$$

Heat is also stored through inertia of the building. The maximum capacity is calculated using simplified method based on ISO 52016-1 [20] as shown in Equation 3.2. The building heat capacity is calculated in Equation 3.3 using the sum of the capacity of its elements, such as internal air, internal walls, and external walls. Referring to values in ISO 52016-1 Table B-14, the internal elements are assumed as class "very light", and external elements as class "medium". The internal air and furniture capacity is defined in ISO 52016-1 Table B-17. The temperature difference for inertia is assumed to be 1°C. The full calculation on building heat capacity is shown in Appendix C.

Table 3.3: Summary of energy supplies

Energy Supply	Price (CHF/kWh)	Emission (kgCO2eq/kWh)	Availability**
Grid Electricity	Figure 3.3		∞
Natural Gas	0.124	0.202	∞
Geothermal	0	0	∞
Solar	0	0	Figure 3.4
Wood	*	0	∞

* Wood price is a variable detailed in Section 3.3.

** Availability implies resource availability at a given time step with ∞ implies sufficiently large energy available to supply the system without it being a constraint.

$$E_{bld}^{stor,cap} = C_{p,bld} \cdot \Delta T \tag{3.2}$$

$$C_{p,bld} = \sum_{i=1}^{N^{bld,el}} c_{p,i} A_i^{ref} \tag{3.3}$$

Thermal network in the heat prosumer community is modelled with low temperature heating pipes at maximum temperature of 50°C. Data from [18] is used to describe the costs associated with installing the pipe. Fix investment is 480CHF/m, variable investment is 0.45CHF/kW/m, and emission is 1kgCO2eq/kW/m. The loss is a variable detailed in Section 3.3.

Table 3.4: Summary of conversion technologies

Conversion Tech.	Capacity Unit	Input	Output	Efficiency	CAPEX (CHF/cap)	OPEX (CHF/cap)	O&M Var. (CHF/kWh)
Gas Boiler	kW	Elec.	ThSH ThDHW	0.93 0.93	243	16	0.0044
GSHP	kW	Elec. + ThSoil	ThSH ThDHW	3.85 2.85	1170	4.5	0
Solar Thermal	m^2	Solar	ThSH ThDHW	0.75 0.55	515	0.21	0
Electric Heater	kW	Elec.	ThSH ThDHW	1.00 1.00	65	1	0.0009
Wood Boiler	kW	Wood	ThSH ThDHW	0.77 0.77	431	34.5	0

Table 3.5: Summary of storage technologies

Storage Tech.	Capacity Unit	Energy Carrier	Max. Cap.	Efficiency (in/out)	Charge Rate (min/max)	Dischr. Rate (min/max)	SoC (min/max)	Standby Loss	CAPEX (CHF/cap)	OPEX (CHF/cap)
DHW Tank	kWh	ThDHW	6	(0.99/0.99)	(0/1)	(0/1)	(0/1)	0.00971	60	0.6
SH Water Tank	kWh	ThSH	18	(0.99/0.99)	(0/1)	(0/1)	(0/1)	0.00971	60	0.6
Building Inertia	kWh	ThSH	15	(1/1)	(0/1)	(0/1)	(0/1)	0.00971	0	0

3.3 Scenarios and Analyses

Table 3.6: Summary of implementation scenarios

Scenarios		Network Loss (1/m)	Technology Candidates	Wood Prices (CHF/kWh)
Base Case (S00)		0	Figure 3.5	-
Set A	Scenario 1 (SA1)	0.01	Figure 3.5	-
	Scenario 2 (SA2)	0.02		
	Scenario 3 (SA3)	0.05		
	Scenario 4 (SA4)	0.08		
	Scenario 5 (SA5)	0.10		
Set B Scenario 1 (SB1)		0	Figure 3.6	-
Set C	Scenario 1 (SC1)	0	Figure 3.7	0.034
	Scenario 2 (SC2)			0.045
	Scenario 3 (SC3)			0.200

The framework described in this study is implemented through three different sets of scenarios. Table 3.6 summarises the scenarios analysed. Three variables are parameterised: thermal pipe network loss, technology candidates in the hubs, and wood pallet prices.

To have a benchmark, a base case is first formulated and analysed. The base case is modelled in ehubX according to the current conditions at nanoverbund as shown in Figure 3.5. The three sets of analyses are devised in this study to answer each preliminary question posted in Section 1.2 respectively. In Set A, the base case is compared with different scenarios where network loss is gradually increased. In Set B, the base case is compared with a decarbonisation strategy of the neighbourhood, where all three houses are given the freedom to choose all technologies except wood boilers. In Set C, the base case is compared with scenarios that introduce wood boilers as alternatives to existing gas boilers at H1 and H3 at different possible prices. In these three scenarios (SC1-SC3), H1 and H3 are also given the flexibility to install more solar thermal collectors in their respective roofs to provide another option for clean conversion technology. Wood price in SC1 is determined from [14]; while in SC2, it is taken from an expert opinion; and in SC3, an extreme high price of 0.2 CHF/kWh for wood is chosen.

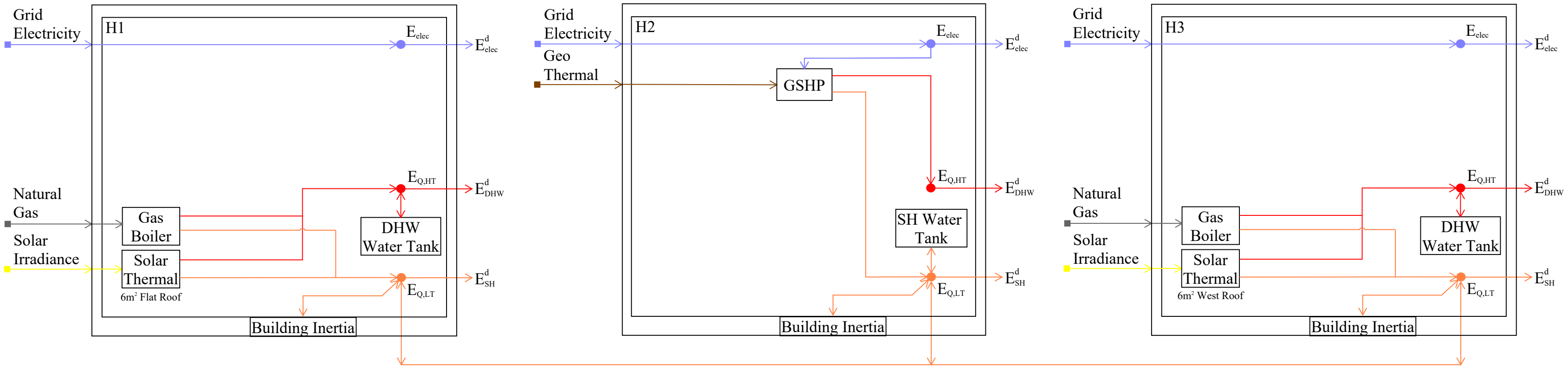

Figure 3.5: Schema of energy system implementation for base case (S00)

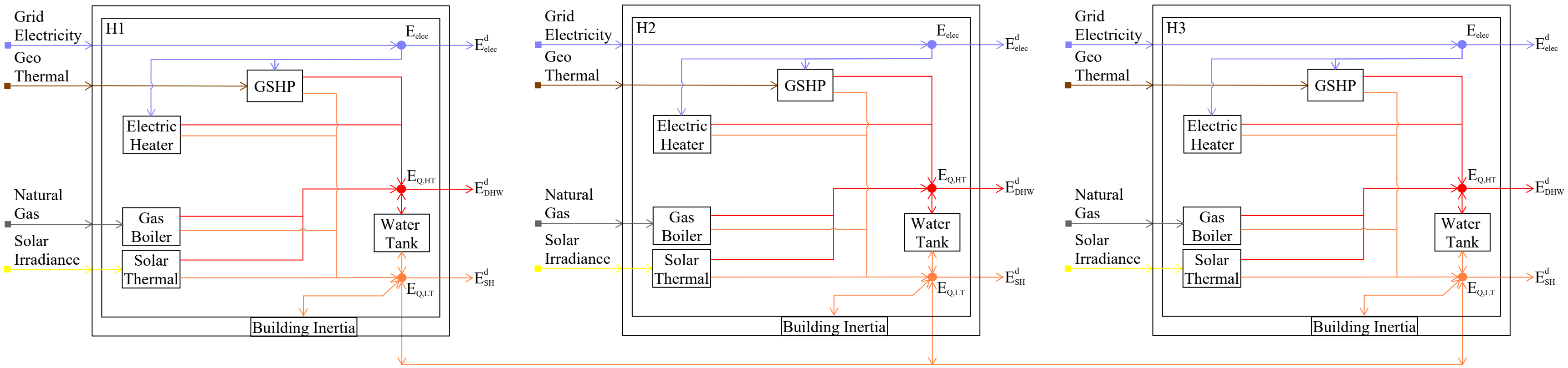

Figure 3.6: Schema of energy system implementations for analysis set B

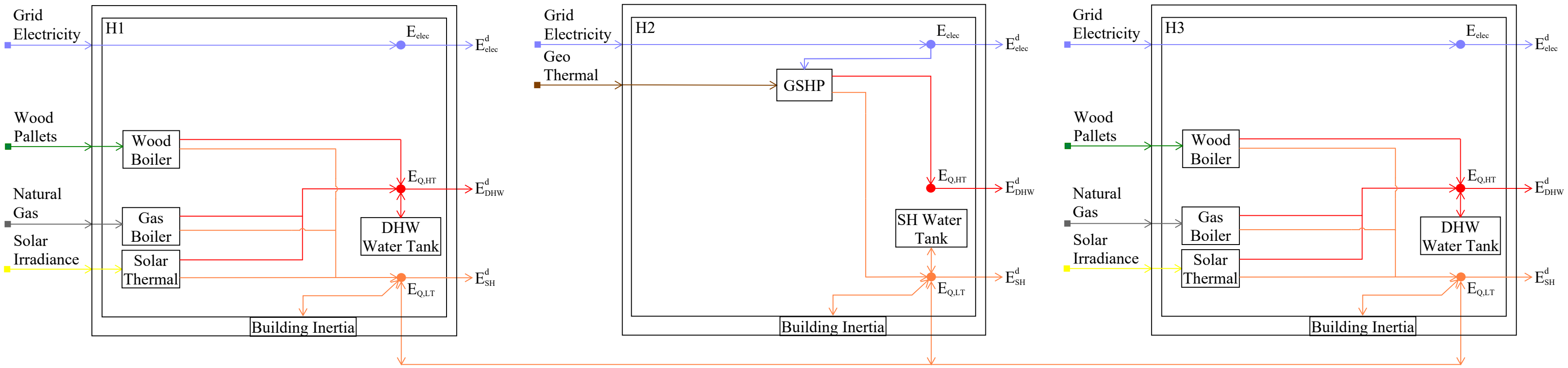

Figure 3.7: Schema of energy system implementations for analysis set C

Chapter 4

Results

The results of the economic and environmental assessment developed for this study are analysed in three separate sets. Each of these sets showcases different trends observed in a heat prosumer community.

4.1 Impacts of Network Loss

Pareto fronts are plotted to show the trade-offs between total cost and total emission of each solution, as shown in Figure 4.1. As devised in Section 2.2, the number of unique solutions for a scenario is set at 4 points plotted within a single Pareto front. For this study, a nomenclature referring to these solutions is created as follows: CO2 efficient for the solution with the lowest total emission, $\varepsilon 1$ and $\varepsilon 2$ are the in-between solutions gradually rising in total emission, and cost efficient for the solution with the lowest total cost. This nomenclature is demonstrated once in Figure 4.1 for solutions of Scenario SA3, and applies to all other sets of solutions for different scenarios. The nomenclature annotations are not repeated for all scenarios for clarity purposes. The Pareto front solution points are also plotted with interpolation lines between them. This representation implies that other solutions can be approximated within the lines in between the explicitly stated four solutions.

Although 4 solutions are inputted as the desired outcome of solving the optimisation problems, several optimisers in some scenarios fail to produce all of them. For example, in S00, SA1, SA2, and SA5, only 3 unique solutions are found. This phenomenon is expected in a mixed integer linear problem with a smaller solution space. In this study, insufficiently diverse technology candidates may be one of the reasons. In the case of Pareto fronts with only 3 solutions, the solutions are named: CO2 efficient, $\varepsilon 1$, and cost efficient.

It is also noted that the linear approximation line between a CO2 efficient solution and $\varepsilon 1$ solution may appear horizontally flat. Numerically, these two solutions still have slight variation in their total emissions. It implies that the optimiser tries to achieve an insignificant total emission reduction in CO2 efficient solution at the expense of large increase in total cost compared to $\varepsilon 1$ solution.

Figure 4.1 shows all the Pareto fronts of the scenarios in Set A. In this analysis set, a clear trend is observed when comparing different scenarios with increasing thermal network loss. The ideal case (S00) with zero loss has the best economic and environmental performances. While for SA5, with 10% loss, the solutions are the worst-performing.

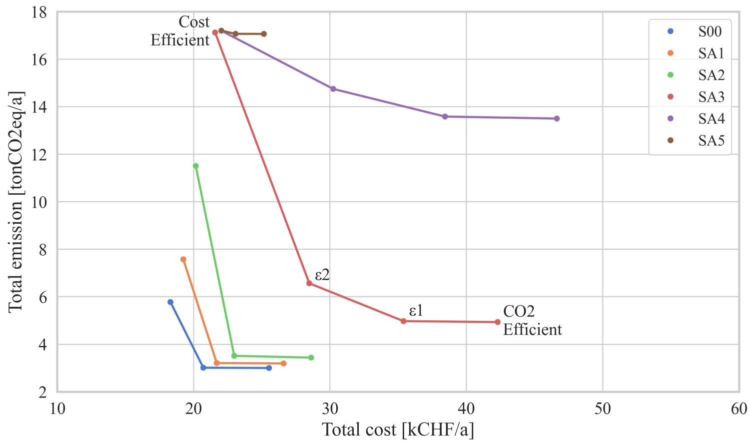

Figure 4.1: Pareto fronts of multi-objective optimisations of scenarios in set A that compare the effect of different network losses. To demonstrate the nomenclature of different solutions in a Pareto front, SA3 Pareto front is annotated with the solution names. These names are generalisable to other Pareto fronts in this study, and are not shown for all fronts for clarity.

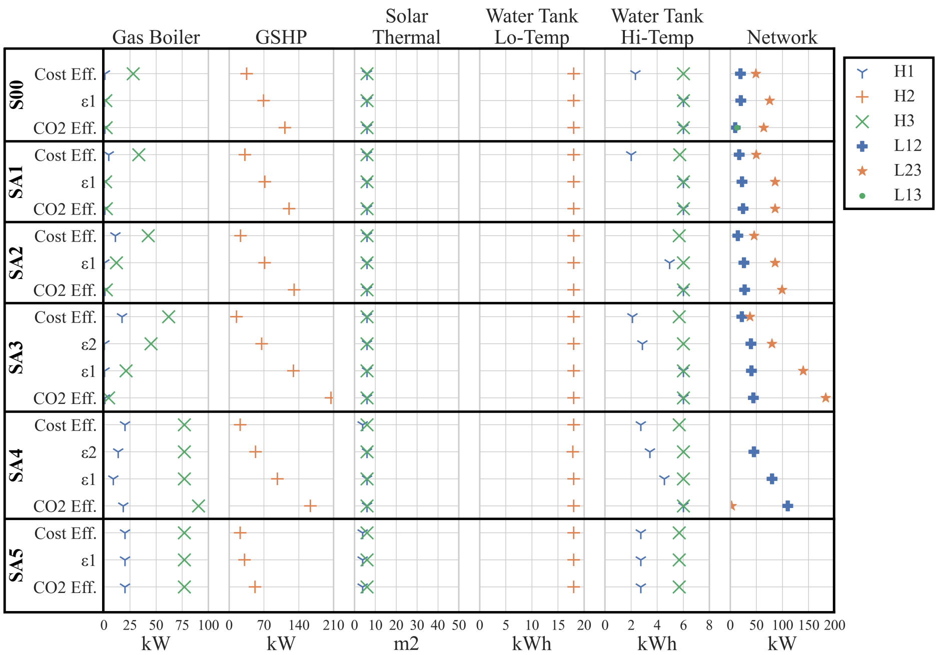

Figure 4.2: Technology capacities selected for all solutions of scenarios in set A. The figure is divided into six columns, each column representing a technology and its capacity installed range, and six major rows for the scenarios, which are further subdivided into their respective solutions. The markers in the cells represent where a technology is installed and are described in the figure legend (top-left).

In terms of technology mixes chosen, Figure 4.2 summarises the installed capacities for solutions in Set A. In all solutions, solar thermal collectors at H1 and H3 and low-temperature water tanks at H2 are almost always installed to the maximum allowed. For solar thermal collectors, the maximum allowed capacities are 6m^2 in both H1 and H3 according to the roof area provided in nanoverbund. Since the installation requires only costs related to initial capacity, without any additional costs on supply imports and subsequent outputs, solar thermal collector at this small size is always a preferable solution. The low-temperature water tank at H2 acts as a complement to the GSHP, which draws its energy supply from an electricity grid that has varying cost and emission. The storage reduces the adverse impacts of these fluctuations, leading to a better optimisation results. Therefore, the optimiser always chooses to install the tank. It is noted that building thermal inertia, which is set as a cost- and emission-free storage technology, is always used in full for all solutions; therefore, it is not shown in the figure for simplicity.

Table 4.1: Annual total network flows for all solutions of scenarios in set A. Lxy indicate flow from hub x to hub y, while Lyx is the reverse. The colours indicate the magnitude of network flows, with red as a larger and green as a smaller flow. An empty cell indicates that a particular flow is not used.

Solutions of Analysis Set A		Annual Network Flow [kWh/a]					
		L12	L21	L23	L32	L13	L31
S00	Cost Eff.	1503	32100	31281	3214		
	ε1	1555	32984	41728	984		
	CO2 Eff.	603	19716	53601	512	2458	14748
SA1	Cost Eff.	820	31997	26042	841		
	ε1	829	35848	41728	984		
	CO2 Eff.	877	35904	46285	29		
SA2	Cost Eff.	991	25035	15135	743		
	ε1	665	40027	53101	15		
	CO2 Eff.	786	40285	53589	23		
SA3	Cost Eff.	1263	2746	3130	1508		
	ε2	657	63171	79308	16		
	ε1	657	64118	100998	16		
	CO2 Eff.	704	64136	101786	12		
SA4	Cost Eff.						
	ε2	622	92594				
	ε1	641	149784				
	CO2 Eff.	708	153669	101786	12		
SA5	Cost Eff.						
	ε1						
	CO2 Eff.						

As the network loss gets higher up to SA3, the crucial technology in the neighbourhood, the GSHP at H2, is gradually decreased in cost-efficient solutions and increased for CO2 efficient solutions. In CO2 efficient solutions, to reduce emission for the neighbourhood, a higher output from GSHP, hence a higher capacity, is needed to compensate increasing heat transfer loss between hubs. This increase, however, is no longer viable in cost efficient solutions since GSHP is one of the most expensive conversion technologies in the neighbourhood. Instead, for these cost efficient solutions, the optimiser chooses to decentralise the energy generation by introducing bigger gas boilers at H1 and H3.

SA4 marks the turning point in CO2 efficient solutions relying on an ever bigger GSHP. As the electricity drawn gets higher due to the losses in the network, total emission from electricity import increases. Burning gas becomes a more desirable conversion method in SA4 and SA5, even for the CO2 efficient solution.

The network capacities installed are following the same trends seen in GSHP installations. For cost efficient solutions, the network is gradually decreased in capacity following the GSHP capacity reduction. While for CO2 efficient solutions, the network is enlarged up to SA3 and then reduced from SA4 onwards. This correlation is the result of the reliance of the whole neighbourhood on H2's GSHP as the main source of clean energy.

High-temperature water tanks are almost always installed to the maximum capacity, 6kWh, at H3 for both cost and CO2 efficient solutions. The same pattern is not seen at H1, where the solutions tend to use less capacities than the solutions at H3. This difference is due to the larger DHW demand at H3 compared to at H1. Another pattern seen in H1 solutions is that the cost efficient solutions tend to install less high-temperature water tank capacity as compared to the CO2 efficient solutions. This observation is related to the gas boiler capacities installed at H1. When a gas boiler is smaller, it does not have the needed capacity to cover higher peak DHW demand. Rather than enlarging the gas boiler, the optimiser deems introducing a larger tank to store heat prior and to release it during peak demand is more economical.

SA5 has the smallest range of Pareto front compared to other scenarios. This result is explained by the lack of any network capacities installed in SA5. In other words, SA5 is no longer a prosumer community and has the same solutions as if the individual hubs were detached. The solutions are not only emission intensive, but also costly, since individual hubs cannot share capacities during peak demand. Limiting network loss in a small-scale, decentralised heat community is, thus, important.

Table 4.1 shows the annual thermal network flow between the three hubs. L12 implies the flow from H1 to H2, while L21 implies the reverse. The same observation that H2 being the important source of clean energy in the neighbourhood is shown in the flow. L21 and L23 are the dominant flows in the thermal network. The reverse flows L12 and L32 are sometimes used during periods where electricity import is more costly or emission intensive than burning gas on-site. As loss grows, this option also fades and becomes less attractive for the solver; it is better for the neighbourhood for H1 and H3 to use their gas boilers on their own demands. L13 and L31 are the least used network, since H1 and H3 technology candidates are almost identical. One exception occurs in CO2 efficient solution for base case scenario S00. Since embodied emission for thermal network is low and the loss is zero, the heat transfer produced in a larger boiler at H3 to H1 becomes possible. However, it is also worth-noting that, as shown in Figure 4.1, the emission saving between the most CO2 efficient solution and the in-between solution ($\epsilon 1$) is negligible. To save a tiny sum of emission, the optimiser opts for investing a lot of cost on additional thermal network.

Figure 4.3 shows the hourly profiles of thermal network flows for cost-efficient and $\epsilon 1$ solutions in base case S00. Thermal network is mainly used during heating period. It is also observed that the network flow profiles in a more CO2 efficient solution fol-

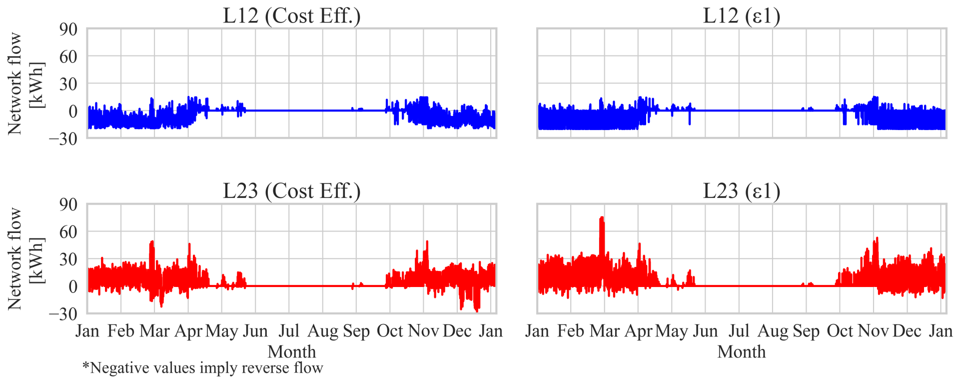

Figure 4.3: Hourly network flows of solutions for base case scenario S00 showing flows between H1 and H2 under cost efficient solution (top-left), flows between H1 and H2 under $\varepsilon 1$ solution (top-right), flows between H2 and H3 under cost efficient solution (bottom-left), and flows between H2 and H3 under $\varepsilon 1$ solution (bottom-right).

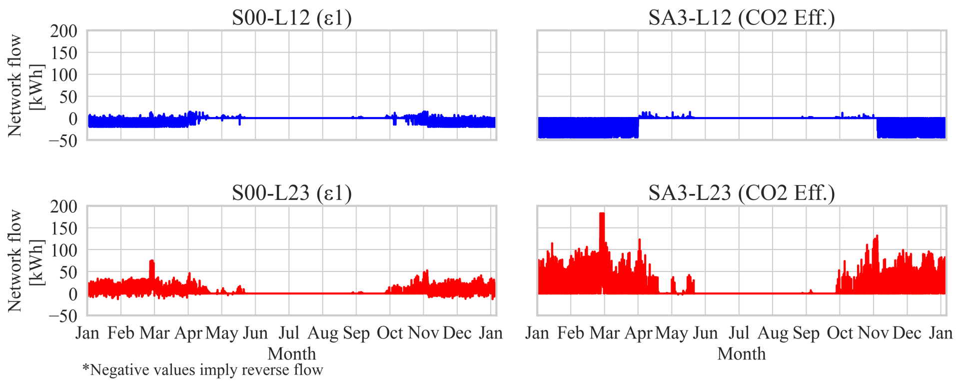

Figure 4.4: Hourly network flows of CO2 efficient solutions showing flows between H1 and H2 in S00 (top-left), flows between H1 and H2 in SA3 (top-right), flows between H2 and H3 in S00 (bottom-left), and flows between H2 and H3 in SA3 (bottom-right).

low the demand profiles of the respective dominant recipient hub, that is L12 in $\varepsilon 1$ follows H1 space heating demand and L23 follows H3 space heating demand. Figure 4.4 shows the comparison of network flow profiles between CO2 efficient solutions in S00 and SA3. The observation regarding similarities with demand patterns is still held with an amplified magnitude due to loss in SA3.

To showcase the interactions between network and storage uses with space heating demand, two heating periods are investigated. In Figure 4.5, profiles on 17-18 November represent typical heating days, where space heating demands amongst the 3 hubs are similar. While in Figure 4.6, an untypical heating period between 26-27 February, where H3 is having an unusually higher space heating demand, is chosen.

In both periods, the network flows are predominantly moving from H2 to H1 and H3. The network flows follow the space heating demand profiles in the respective hubs. The effect of network loss is clearly seen in the amplified magnitude of SA3

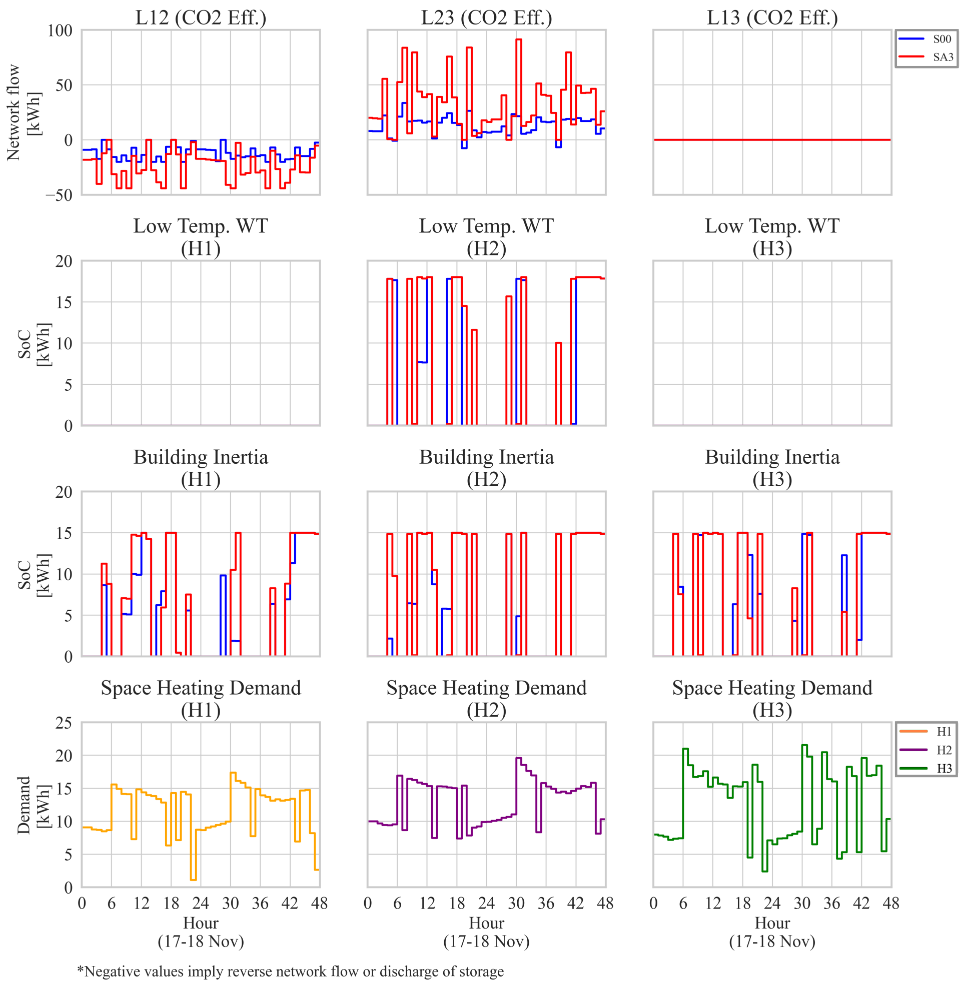

Figure 4.5: Network flows, storage SoCs, and demand profiles during two consecutive typical heating days (17-18 November).

thermal network compared to S00. In scenario SA3, storages are used more to anticipate future demand. The state of charge (SoC) of SA3 storages are more often at the maximum and drawn abruptly to meet demand on the hour.
An anomaly is noted for H1's building inertia in S00 at 1200-2400 on the 26 February. At these hours, there is no space heating demand from H1, yet heat is still drawn from the inertia. This is due to the inaccurate modelling of building inertia that is coupled with ThSh, an energy carrier that is also applied to the thermal network. At the same period, a small amount of heat is flowing in L12, which implies heat is drawn from this inertial storage to fulfil demand in other hubs. When loss is high in SA3, this behaviour is not observed, as the optimiser is dissuaded to transfer heat with unnecessary loss.

It is noted that some demand profiles are counter-intuitive to typical perceptions of space heating needs. For example, the demand is oscillating quite abruptly within the span of only two hours. This behaviour is explained by the demand datasets that are generated from converted electrical responses of heat pumps using a constant COP. There are also hours when H1 and H2 have zero demands. This phenomenon is approximated to a real-life situation where for one reason or another the heating

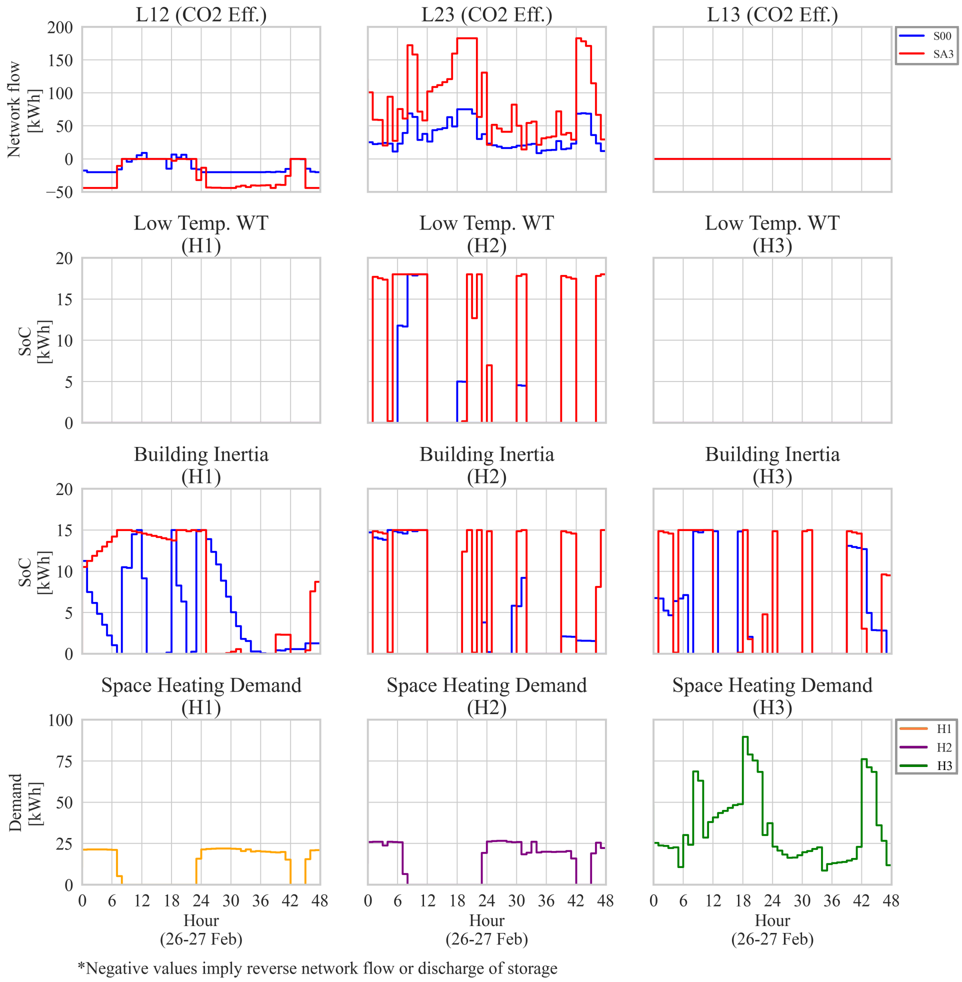

Figure 4.6: Network flows, storage SoCs, and demand profiles during two consecutive unusual heating days (26-27 February).

systems are forced to be turned off. As this study focuses to showcase a general study on network responses to any demand profiles, the anomalies spotted in the demand datasets are deemed acceptable.

4.2 Impacts of Individual Hub Decarbonisation

As observed in the analyses of Set A, having a hub in the neighbourhood as the main clean energy source plays a pivotal role in choosing to install networks. In Set B, the impacts of decarbonising all hubs in the neighbourhood are analysed. Figure 4.7 shows the Pareto fronts of base case S00 and SB1. Compared to S00, SB1 shows reductions in emissions for both cost efficient solution and CO2 efficient solution. While for the former solution, cost does not differ much from S00's solution, SB1's CO2 efficient solution comes at a substantial increase in total cost.

The technologies chosen and their capacities in analysis set B are summarised in Figure 4.8. Overall, it can be seen that thermal network is used less in SB1 com-

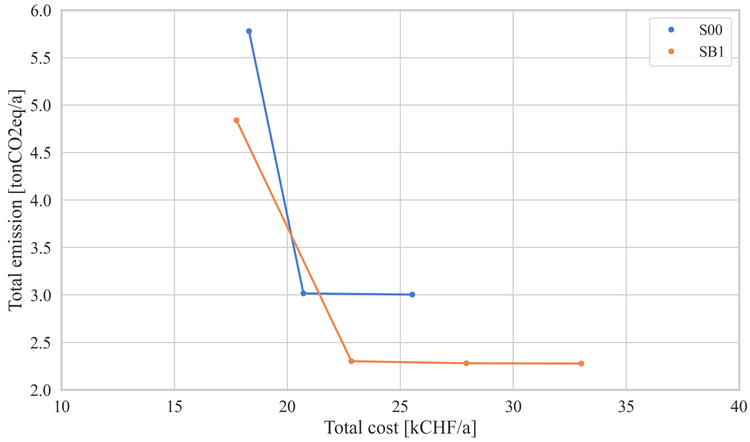

Figure 4.7: Pareto fronts of multi-objective optimisations of scenarios in set B that compare the effect of full energy decarbonisation of all hubs in the community.

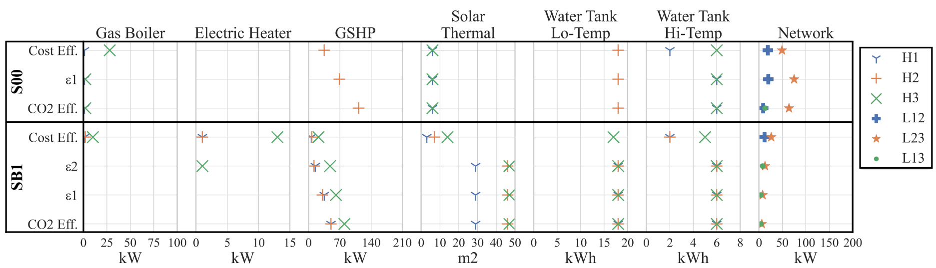

Figure 4.8: Technology capacities selected for all solutions of scenarios in set B. The figure is divided into seven columns, each column representing a technology and its capacity installed range, and two major rows for the scenarios, which are further subdivided into their respective solutions. The markers in the cells represent where a technology is installed and are described in the figure legend (top-left).

pared to S00. The freedom given to the optimiser to select numerous technologies in respective hubs creates fewer needs for a network. In the cost-efficient solution, SB1 reduces the dependency on using GSHP by installing new electric heaters and more solar thermal collectors. The switch from an expensive GSHP to other cheaper technologies explain the slight reduction in cost compared to S00. Low temperature water tank is also installed at H3 instead of H2, which is due to H3 being the largest consumer and hosting larger conversion technology capacities in this solution.

Table 4.2: Annual total network flows for all solutions of scenarios in set B. Lxy indicate flow from hub x to hub y, while Lyx is the reverse. The colours indicate the magnitude of network flows, with red as a larger and green as a smaller flow. An empty cell indicates that a particular flow is not used.

Solutions of Analysis Set B		Annual Network Flow [kWh/a]					
		L12	L21	L23	L32	L13	L31
S00	Cost Eff.	1503	32100	31281	3214		
	ε1	1555	32984	41728	984		
	CO2 Eff.	603	19716	53601	512	2458	14748
SB1	Cost Eff.	2809	14253	4798	30544		
	ε2			6221	12807	4030	9530
	ε1			6517	6434	4244	5366
	CO2 Eff.			5637	4281	4213	4501

As the optimiser progresses to find a more CO2 efficient solution, a GSHP becomes more attractive compared to an electric heater due to its higher COP. Due to its zero operational emissions, solar thermal collectors are applied in all available roof areas in all three hubs. Provided with enough clean energy sources in individual hubs, the thermal network becomes increasingly redundant in the CO2 efficient solution of SB1. However, the excessive installation of various technologies in each hub to pursue slightly lower emissions causes the substantial increase in total cost compared to S00.

Additional attentions need to be given in implementing this study framework with its all-options-available approach. Technology area constraints, except for those of the solar technologies, are not yet implementable in ehubX. Although Set B in this study demonstrates the extreme boundary of such condition, the solutions provided may not be applicable to real life design. For example, a single family house may not be able to host three different boilers and a GSHP.

Table 4.2 shows the annual network flows in this set. Compared to S00, the neighbourhood in SB1 gravitates toward H3 as a source of energy. It can be inferred by the large network flow from L32 and L31. In the cost efficient solution, the fixed cost of installing a longer L31 when L32 has been installed is not preferred. The better solution is to transfer the heat through H2, then to H1. It needs to be noted that this solution is feasible due to zero network loss. While, when fixed cost is no longer the concern as in CO2 efficient solution, heat is transferred mainly from and through H3.

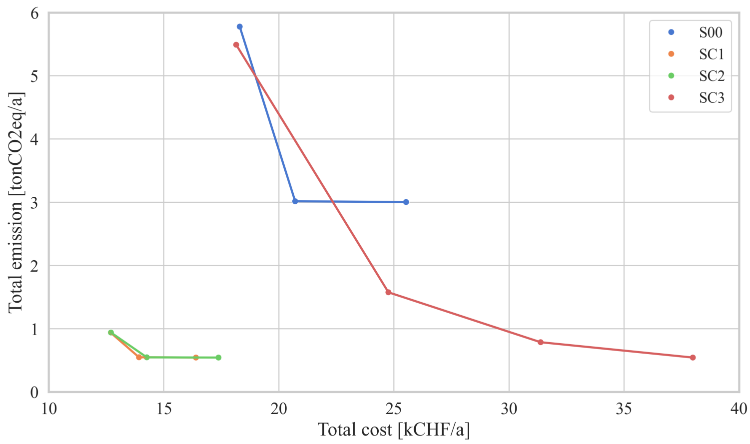

Figure 4.9: Pareto fronts of multi-objective optimisations of scenarios in set C that compare the effect of the introduction of wood heating sources at different price points.

4.3 Impacts of Increasing Wood Prices

Another source of less emission-intensive conversion technology not yet explored in Set A and B is a wood boiler. The impacts of introducing such technology are analysed in Set C. As shown in Figure 4.9, introducing wood boilers at H1 and H3 at low prices in SC1 and SC2 shifts the Pareto fronts significantly lower compared to S00. Subsequently, as shown in Figure 4.10, large wood boilers are installed at H1 and H3, while GSHP at H2 is no longer preferred. In these two scenarios' cost-efficient solutions, gas boilers and solar thermal collectors are installed at H1 and H3 alongside the wood boilers. The combination of these three conversion technologies provide the cheapest solution for the neighbourhood. It is also shown that the Pareto fronts between SC1 and SC2 does not differ too much. The wood price increase from 0.034CHF/kWh to 0.045CHF/kWh is not significant enough to cause major increases in either cost or emission. The optimiser manages to adapt to the price increase with minor adjustments, such as placing a larger wood boiler at H3, but eliminating the wood boiler at H1; increasing the network capacity slightly; and introducing a larger gas boiler at H1.

When the wood price is increased extremely as modelled in SC3, wood boilers are no longer cost-viable solutions. The technology mixes of SC3 in a cost-efficient solution is similar to that of the S00. As the optimiser moves towards minimising emission, a wood boiler with its zero operational emission is chosen once more. Although emissions in these solutions of SC3 are lower than that of S00, the total costs are significantly higher. It is also worth-noting that unlike in SC1 and SC2, more solar thermal collectors are installed in SC3. It becomes viable to spend upfront installation costs of thermal collectors, which does not require additional operational costs, to alleviate the necessity of importing expensive wood.

Table 4.3 summarises the annual network flows for solutions in Set C. In cost-effective solutions where wood is relatively cheap (SC1 and SC2), H3 through network flow L32 is the main source of energy for the neighbourhood. This is in contrast to solutions in S00 and in SC3 when wood is expensive, where the energy is once again mainly drawn from H2 through L21 and L23. For CO2 efficient solutions, it is noted that the network in and out of H3 is no longer selected. The

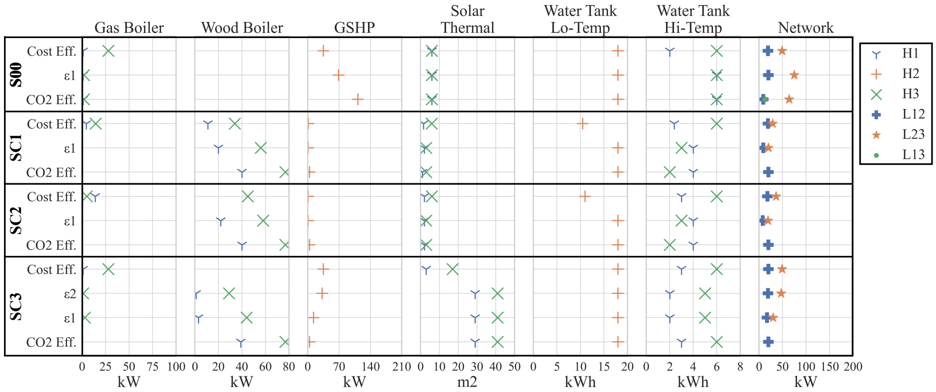

Figure 4.10: Technology capacities selected for all solutions of scenarios in set C. The figure is divided into seven columns, each column representing a technology and its capacity installed range, and four major rows for the scenarios, which are further subdivided into their respective solutions. The markers in the cells represent where a technology is installed and are described in the figure legend (top-left).

optimiser chooses to allow H3 to fulfil its own needs without providing for other hubs. H2 is still receiving heat generated by the wood boiler at H1. The significant switch between the in-between solutions $\varepsilon 1$ and CO2 efficient solutions renders the latter solutions trivial. As seen in the Pareto fronts in Figure 4.9, the reduction in emission is unnoticeable, with significant cost increases as trade-offs. Providing networks in between the three hubs may still be the better option.

Table 4.3: Annual total network flows for all solutions of scenarios in set C. Lxy indicate flow from hub x to hub y, while Lyx is the reverse. The colours indicate the magnitude of network flows, with red as a larger and green as a smaller flow. An empty cell indicates that a particular flow is not used.

Solutions of Analysis Set C		Annual Network Flow [kWh/a]					
		L12	L21	L23	L32	L13	L31
S00	Cost Eff.	1503	32100	31281	3214		
	ε1	1555	32984	41728	984		
	CO2 Eff.	603	19716	53601	512	2458	14748
SC1	Cost Eff.	1513	4577	1239	38215		
	ε1	10640	7672	3855	27861		
	CO2 Eff.	34147	0				
SC2	Cost Eff.	432	30674	776	64924		
	ε1	647	21396	685	55776		
	CO2 Eff.	34422	77				
SC3	Cost Eff.	1349	32938	29981	5982		
	ε2	2837	27570	20261	22144		
	ε1	3020	20897	7367	44094		
	CO2 Eff.	34892	8				

Chapter 5

Conclusions and Discussion

5.1 Conclusions

This study develops an initial framework for assessing the economic and environmental viability of a decentralised heat prosumer community. A multi-energy multi-hub model is created using ehubX tool, developed by Empa. The model is capable of solving a multi-objective minimisation problem between costs and emissions on a three-hub neighbourhood connected by low-temperature heat networks. The study mainly addresses heat conversion and storage technologies related to space heating and DHW demands. An accurate modelling of two COPs within the same heating device that provides both low and high temperatures are presented. As electricity is not the main focus of this study, the neighbourhood electricity demands, heat pump and electric boiler electricity needs are fulfilled wholly by the electricity grid.

The framework mentioned is applied to a case study involving three thermally connected single family houses in Basel under the nanoverbund project. The implementations answer three questions:

1. Q: How does thermal network loss impacts the deployment of that system in a heat prosumer community?

   A: Network loss plays significant roles in determining whether installing networks in the neighbourhood makes economic and environmental sense. With the base case initial conditions, which are modelled according to nanoverbund, 10% loss is found to be the approximate threshold when networks are no longer preferable. Cost- and emission-efficient solutions diverge in their technology installed as loss increases. This question is answered in Section 4.1.

2. Q: What are the technologies installed if all hubs in the community were given the same technology candidates to decarbonise?

   A: Given equal technology candidates for decarbonisation in each individual house, installing a network in the neighbourhood is no longer the most preferable option. Although it is noted that installing multiple technologies is not practically feasible in small houses, this question still signifies the importance of variations in solving optimisation problems with linked hubs. In this set of scenarios, the variations in technology candidates are eliminated. This question is answered in Section 4.2.

3. Q: With increasing popularity of wood boilers, does it still make sense to use them in the community if prices were to rise in the future?

   A: Wood boilers are disruptors in the optimisation of the community. With zero operational emission and low prices, the optimiser is almost certain to choose these boilers compare to other technologies. Wood price is increased to mimic market responses to an increase in wood demand. It is shown that the framework is able to capture the effects of this situation, with a tendency to choose wood boilers at low prices and a return towards base case technology selections once wood is no longer economical. This question is answered in Section 4.3.

5.2 Limitations and Outlook

In applying energy optimisation on a smaller scale, selection of multiple technologies may pose dissimilar constraints as that of on a larger scale. ehubX library developed by Empa's Urban Energy System Lab is capable in developing most of the challenges presented in designing this project. However, it still lacks the capability to introduce floor area occupied by non-solar technologies constraints. It limits the practical design feasibility of the solutions to a problem that generalises the implementations with multiple technology candidates, as shown in Section 4.2 in this study.

It is also acknowledged that this study does not model directly building demands of nanoverbund due to the interest of time. Although the used demand datasets are approximated well to fit the case study, the thermal profiles gathered are post-processing results of heat pump responses made for other studies. This condition may influence the results and profiles calculated for networks and storages discussed in Section 4.1.

The embodied emissions of all technologies have not been taken into considerations in this study. It is deemed by the author that the embodied emissions of three small houses in a neighbourhood are not the deciding factor in technology selections. The dataset for the emissions for smaller devices are more difficult to obtain. However, it is important to note that for a fairer comparison, embodied emissions should be taken into considerations. The general framework itself is not affected by this limitation, since introducing embodied emissions only means changing certain input values in the implementations.

Recommendations on improvements for the economic and environmental assessment framework in this study:

1. Introduce embodied emissions of technologies.
2. Introduce space cooling demands and respective cooling technologies.
3. Introduce more complexities to the implementations, such as options for ThDHW pipes that are coupled with ThSh pipes, PV panels, home batteries, and electrical lines between houses.
4. Improve the accuracy of GSHP modelling with seasonal storages through boreholes and full regeneration of ground heat.
5. Investigate further the accuracy of modelling a virtual storage technology, such as building thermal inertia.

6. Formulate rough correlation of floor area used to technology capacity to provide pseudo-area-constraints.

Future works envisaged for broader implementations on the assessments on heat prosumer communities:

1. Investigate through proper sensitivity analyses of different parameters affecting implementation feasibility of a heat prosumer oriented community, such as demand profiles, network loss, technology availability, prices and carbon intensities of energy carriers.

2. Quantifying shadow pricing for the social benefits gained by introducing the network pipes.

3. Explore neighbourhood reliance to disruptions as another metric to evaluate the benefits of implementing such heat prosumer community concept.

Chapter 6

Acknowledgements

This project is developed based on an ongoing SWEET PATHFNDR and EDGE pilot project in Basel, specifically the nanoverbund project. The author would like to express special thanks to direct supervisors of this project, Dr. Hanmin Cai, Dr. Binod Prasad Koirala, and Prof. Dr. Philipp Schütz, whose helps made the success of this project possible; to colleagues at Empa, especially Dr. Gabriele Humbert and Matthias Brandes, who have given access to various datasets; to colleagues at HSLU, especially Dr. Curtis Meister, who has shared his heat capacity calculations; to Prof. Dr. Matthias Sulzer who introduced the author to Sympheny platform in ETH course of Building Systems II; to Josein de Koning and Florian Bürgler, whose project reports and ehubX implementations inspire this project; and finally to Prof. Dr. Gabriella Hug who examines and supports this semester project.

Bibliography

[1] European Environment Agency, *Energy prosumers in Europe – Citizen participation in the energy transition.* Publications Office of the European Union, 2022.

[2] D. Frieden and A. Tuerk, "Regulatory frameworks for energy communities in the pilot site countries croatia, spain, greece, portugal and slovenia shaping eu framework transposition and project implementation (deliverable 2.3)," 10 2020.

[3] Schoonschip. (2023) Schoonschip amsterdam - introduction energy.

[4] Cooperativa Som Energia. (2023) How does simplified surplus compensation work?

[5] A. Nouicer, A. Kehoe, J. Nysten, D. Fouquet, L. Meeus, and L. Hancher, *The EU clean energy package – (2020 ed.).* European University Institute, 2020.

[6] Swiss Federal Office of Energy, "Energy strategy 2050 once the new energy act is in force," Jan 2018.

[7] D. B. der Schweizerischen Eidgenossesnschaft, "Energiegesetz 730.0," Tech. Rep., 2016.

[8] Swiss Federal Office of Energy, "In 2022, two-thirds of households were heated by fossil fuels," *Buildings and Dwellings Statistics 2022*, Sep 2023.

[9] P. Zeniewski, G. Molnar, and P. Hugues, "Europe's energy crisis: What factors drove the record fall in natural gas demand in 2022?" Mar 2023.

[10] Swiss Federal Office of Energy, "Energy – facts and figures," Feb 2023.

[11] L. Horstink, G. Luz, M. Soares, and K. Ng, "Review and characterisation of collective renewable energy prosumer initiatives (deliverable 2.1)," 05 2019.

[12] Gurobi Optimization, LLC, "Gurobi Optimizer Reference Manual," 2023.

[13] Q. Li, N. Vulic, H. Cai, and P. Heer, "Flexibility implications of optimal pv design: building vs. community scale," *Journal of Physics: Conference Series*, vol. 2600, no. 8, p. 082002, nov 2023.

[14] T. Marti, M. Sulzer, M. Rüdisüli, C. Opitz, E. Romano, J. Marquant, K. Orehounig, M. Yazdanie, M. Schuerle, N. Vulic, P. Heer, R. Mutschler, S. Eggimann, Y. Sherif, and U. Elber, "Energieversorgung der schweiz bis 2050 zusammenfassung von ergebnissen und grundlagen," 12 2022.

[15] ENTSO-E, "Entso-e transparency platform," 2022.

[16] D. B. C. Lawrie, Linda K, "Development of global typical meteorological years (tmyx)," 2022.

[17] C. Waibel, R. Evins, and J. Carmeliet, "Efficient time-resolved 3d solar potential modelling," *Solar Energy*, vol. 158, pp. 960–976, 2017.

[18] HSLU, "Heizkostenvergleichsrechner v035," Tech. Rep., 2021.

[19] S. B. M. E. Matthias Bethold, Michael Uhlmann, "Feldmessungen von wärmepumpen-anlagen heizsaison 2021/22," HSLU, Tech. Rep., 2022.

[20] D. van Dijk, "En iso 52016-1: The new international standard to calculate building energy needs for heating and cooling, internal temperatures and heating and cooling load," 01 2019, pp. 4061–4068.

[21] P. Huber, M. Ott, M. Friedli, A. Rumsch, and A. Paice, "Residential power traces for five houses: The ihomelab rapt dataset," *Data*, vol. 5, no. 1, 2020.

[22] M. Schlemminger, T. Ohrdes, E. Schneider, and M. Knoop, "Dataset on electrical single-family house and heat pump load profiles in germany," *Scientific Data*, vol. 9, no. 1, 2022.

[23] P. Schuetz, A. Melillo, F. Businger, R. Durrer, S. Frehner, D. Gwerder, and J. Worlitschek, "Automated modelling of residential buildings and heating systems based on smart grid monitoring data," *Energy and Buildings*, vol. 229, p. 110453, 2020.

[24] "Raumnutzungsdaten für die energie- und gebäudetechnik," Swiss Society of Engineers and Architects, Zurich, CH, Standard, oct 2015.

[25] L. G. Swan and V. I. Ugursal, "Modeling of end-use energy consumption in the residential sector: A review of modeling techniques," *Renewable and Sustainable Energy Reviews*, vol. 13, no. 8, pp. 1819–1835, 2009.

[26] S. A. Klein, W. A. Beckman, and P. I. Cooper, *TRNSYS: A transient simulation program.* University of Wisconsin, 1978.

[27] SEL, *TRNSYS 18: a TRaNsient SYstem Simulation program*, Solar Energy Laboratory University of Wisconsin–Madison, 2023, available at https://sel.me.wisc.edu/trnsys/features/trnsys18_0_updates.pdf.

[28] D. Robinson, F. Haldi, P. Leroux, D. Perez, A. Rasheed, and U. Wilke, "Citysim: Comprehensive micro-simulation of resource flows for sustainable urban planning," 07 2009.

[29] N. Björsell, A. Bring, L. Eriksson, P. Grozman, M. Lindgren, P. Sahlin, A. Shapovalov, and M. Vuolle, "Ida indoor climate and energy," in *Proc. of the 6-th IBPSA Conference.* Citeseer, 1999, pp. 1035–1042.

[30] C. F. Reinhart, T. Dogan, J. A. Jakubiec, T. Rakha, and A. Sang, "Umi-an urban simulation environment for building energy use, daylighting and walkability," 2013.

[31] D. Wang, J. Landolt, G. Mavromatidis, K. Orehounig, and J. Carmeliet, "Cesar: A bottom-up building stock modelling tool for switzerland to address sustainable energy transformation strategies," *Energy and Buildings*, vol. 169, pp. 9–26, 2018.

[32] P. Nageler, G. Zahrer, R. Heimrath, T. Mach, F. Mauthner, I. Leusbrock, H. Schranzhofer, and C. Hochenauer, "Novel validated method for gis based automated dynamic urban building energy simulations," *Energy*, vol. 139, pp. 142–154, 2017.

[33] D. B. Crawley, L. K. Lawrie, C. O. Pedersen, and F. C. Winkelmann, "Energy plus: energy simulation program," *ASHRAE journal*, vol. 42, no. 4, pp. 49–56, 2000.

[34] J. A. Fonseca and A. Schlueter, "Integrated model for characterization of spatiotemporal building energy consumption patterns in neighborhoods and city districts," *Applied Energy*, vol. 142, pp. 247–265, 2015.

[35] B. Howard, L. Parshall, J. Thompson, S. Hammer, J. Dickinson, and V. Modi, "Spatial distribution of urban building energy consumption by end use," *Energy and Buildings*, vol. 45, pp. 141–151, 2012.

[36] J. Mikkola and P. D. Lund, "Models for generating place and time dependent urban energy demand profiles," *Applied Energy*, vol. 130, pp. 256–264, 2014.

[37] H.-M. Groscurth, T. Bruckner, and R. Kümmel, "Modeling of energy-services supply systems," *Energy (Oxf.)*, vol. 20, no. 9, pp. 941–958, Sep. 1995.

[38] Intergovernmental Panel on Climate Change, *Climate change 2014: Mitigation of climate change.* Cambridge, England: Cambridge University Press, Jan. 2015.

[39] M. Geidl, G. Koeppel, P. Favre-Perrod, B. Klöckl, G. Andersson, and K. Fröhlich, "The energy hub-a powerful concept for future energy systems," *Third Annual Carnegie Mellon Conference on the Electricity Industry*, pp. 13–14, 04 2007.

[40] R. Evins, K. Orehounig, V. Dorer, and J. Carmeliet, "New formulations of the 'energy hub' model to address operational constraints," *Energy*, vol. 73, pp. 387–398, 2014.

[41] K. Orehounig, R. Evins, and V. Dorer, "Integration of decentralized energy systems in neighbourhoods using the energy hub approach," *Applied Energy*, vol. 154, pp. 277–289, 2015.

[42] L. A. Bollinger and V. Dorer, "The ehub modeling tool: A flexible software package for district energy system optimization," *Energy Procedia*, vol. 122, pp. 541–546, 2017, cISBAT 2017 International ConferenceFuture Buildings Districts – Energy Efficiency from Nano to Urban Scale.

[43] L. A. Bollinger, J. Marquant, and M. Sulzer, "Optimization-based planning of local energy systems -bridging the research-practice gap," *IOP Conference Series: Earth and Environmental Science*, vol. 323, p. 012077, 09 2019.

[44] Sympheny. (2023) Sympheny user guide.

[45] J. A. Fonseca, T.-A. Nguyen, A. Schlueter, and F. Marechal, "City energy analyst (cea): Integrated framework for analysis and optimization of building energy systems in neighborhoods and city districts," *Energy and Buildings*, vol. 113, pp. 202–226, 2016.

[46] H. Li, J. Hou, Z. Tian, T. Hong, N. Nord, and D. Rohde, "Optimize heat prosumers' economic performance under current heating price models by using water tank thermal energy storage," *Energy*, vol. 239, p. 122103, 2022.

[47] D. Keiner, M. Ram, L. D. S. N. S. Barbosa, D. Bogdanov, and C. Breyer, "Cost optimal self-consumption of pv prosumers with stationary batteries, heat pumps, thermal energy storage and electric vehicles across the world up to 2050," *Solar Energy*, vol. 185, pp. 406–423, 2019.

[48] B. Manrique Delgado, R. Kotireddy, S. Cao, A. Hasan, P.-J. Hoes, J. L. Hensen, and K. Sirén, "Lifecycle cost and co2 emissions of residential heat and electricity prosumers in finland and the netherlands," *Energy Conversion and Management*, vol. 160, pp. 495–508, 2018.

[49] P. Huang, M. Lovati, X. Zhang, C. Bales, S. Hallbeck, A. Becker, H. Bergqvist, J. Hedberg, and L. Maturi, "Transforming a residential building cluster into electricity prosumers in sweden: Optimal design of a coupled pv-heat pump-thermal storage-electric vehicle system," *Applied Energy*, vol. 255, p. 113864, 2019.

[50] B. P. Koirala, J. P. Chaves Ávila, T. Gómez, R. A. Hakvoort, and P. M. Herder, "Local alternative for energy supply: Performance assessment of integrated community energy systems," *Energies*, vol. 9, no. 12, 2016.

[51] B. Koirala, R. Mutschler, A. Bartolini, A. Bollinger, and K. Orehounig, "Flexibility assessment of e-mobilty in multi-energy districts," in *CIRED Porto Workshop 2022: E-mobility and power distribution systems*, vol. 2022, 2022, pp. 824–828.

Appendix A

Literature Review

A.1 Building Energy Demand

Building energy demand profiles are one of the key information needed in built engineering design. The accuracy of deriving these profiles determines the effectiveness of the design interventions, ranging from energy supply management to building component sizing. Within this study, gathering representative energy demand profiles from individual buildings in the decentralised heat prosumer communities is an essential first step. Therefore, selected methods of generating these demand profiles are reviewed.

Direct measurement

Direct measurement in an operational building is one straightforward way to gather energy demand profiles. Recent advancements in inexpensive sensor and data storage technologies have made this method feasible to be deployed in investigating several buildings.

One study performed direct measurements on five dwellings in the greater Lucerne area for periods ranging from 1.5 to 3.5 years [21]. The houses were equipped with several meters detecting the electricity loads of appliances, heat pumps, total grid consumption, and photovoltaic (PV) generation with sampling time of five minutes.

In another study [22], 38 single family houses in Lower Saxony, Germany were measured for their household and heat pump electricity consumption. The data was collected in a span of 2.5 years with temporal resolution of 10 seconds to 60 minutes.

Energy consumption measurement is also done on a grid level. One study [23] introduces an algorithm that translates this macro-level measurement into estimated characteristic values of constituent buildings. The resulting building physical properties are then used to predict each building demand.

Standard values

A code of practice in engineering is a written document developed by a professional body or government agency to standardise and prescribe best practices in the industry. The document is intended to provide practitioners practical and safe ways in designing a project at hand.

In Switzerland, SIA2024 by the Swiss Society of Engineers and Architects (SIA) is the code of practice in determining building energy demand [24]. There are 45 use typologies defined by the standard that covers residential, commercial, industrial, and public uses. The energy demand values are normalised by net conditioned area of the corresponding use per year. The demand profile is then derived from these figures with the provided schedule of use.

Bottom-up modelling approach

Building energy modelling (BEM) is categorised into two distinct approaches: bottom-up and top-down [25]. The first type of modelling considers estimating an energy consumption through creating a representative set of parameters that behaves similarly to the building under investigation. These parameters consist of geometric and non-geometric properties of the building.

One method to perform bottom-up modelling approach is a physics-based method. Transient System Simulation (TRNSYS) [26] was one of the first powerful tools developed for physics-based BEM using Fortran Programming Language. The tool provides the ability to model a detailed multi-zone building. The minimum inputs required by the tool are construction types, glazing types, building schedules, heating, ventilation, and air conditioning (HVAC) regime types, air node definition, and weather file [27]. The output is a comprehensive report ranging from indoor comfort performances to hourly demand profiles.

Since the development of TRNSYS, multiple BEM tools have emerged with their own distinctive features. One recent advancement in this topic stems from the need to model not only individual buildings, but to include urban spatial boundaries. Selected tools are presented in this study: CITYSIM [28], IDA Indoor Climate and Energy (IDA ICE) [29], Umi [30], and Combined Energy Simulation And Retrofitting (CESAR) [31].

With CITYSIM [28], building energy, embodied carbon, water, and waste flows are its central features. It scales well from a few buildings up to a medium-sized neighbourhood. The tool implements an evolutionary model that can derive the hourly cooling and heating demand flows between buildings. In [32], IDA ICE is coupled with Geographic Information System (GIS)-based method that automates the data extraction process of an urban setup. The tool is intended to model a multi-building district through defined typologies and project databases. The resulting urban model is then solved using physics-based methods proposed in the original IDA ICE [29]. One notable output from this tool is an hourly district heating power consumption profile. To answer the growing needs of new large-scale urban developments, Umi [30] was developed. The tool uses Rhinoceros, a (Computer-Aided Design) CAD programme, for its geometric inputs and Daysim for daylight simulation. These inputs combined with building information are fed to Energy Plus solver [33] to physically simulate the urban setup. Hourly electricity, gas use, and carbon emission of the district are extracted as possible outputs of this tool. The CESAR tool [31] was developed to address district retrofitting strategies in Switzerland. The tool comprises demand model and retrofitting model. In the first part, CESAR uses GIS and archetypal approach in defining individual buildings in the district. Simplifications are then made to assume one energy zone per floor of a building. The physics-based solver used is Energy Plus [33]. The output of the demand model is hourly energy demand profiles that consider district interactions.

Apart from physics-based method, some demand forecasting models combine this method with a statistical approach. In one tool, City Energy Analyst (CEA) [34], aims to perform demand forecasting of an urban area using analytical approaches for energy flow and temperatures, and statistical approaches to scale it up for yearly consumption. The tool simplifies building geometries to one energy zone and groups similar buildings into an archetype. The model yields hourly energy demands for each building and aggregates them on a district level. The hybrid approach allows determination of spatio-temporal variability of energy demands for existing and future buildings.

Top-down modelling approach

Another approach in determining energy consumption is top-down modelling. This approach is intended to provide a tractable way of estimating energy uses on a larger scale. Stochastic methods are utilised in this approach.

In [35], the annual New York City wide energy consumption in 2009 was determined. The estimation was performed based on building functions, in contrast to the traditional physics-based approach using construction types. The inputs, statistics of previous years' electricity and fuel use, are described in eight functions. Robust multiple linear regressions are performed on these functions to develop the output of end-use energy intensity.

Another example of this approach is the use of transformation of past temporal load data into spatio-temporal form [36]. The temporal load is split into three consumer classes: households, services, and industry. Using the exponential density model, these load profiles are further decomposed into their spatio-temporal forms. The output is a spatial distribution of energy consumption intensity of a district. The method had been applied to two different urban setups in Helsinki and Shanghai.

A.2 Energy System Design

The relations between various interconnected buildings with their demands, multiple energy sources, and the technologies that facilitate the transfer of energy between the two constitutes an energy system [37]. The Intergovernmental Panel on Climate Change (IPCC) formally defines the system as all components that produces, converts, delivers, and uses energy [38]. With the complexity in optimally designing such system, several tools are developed to address the problem.

One concept for energy system design developed in[39] is called an energy hub. The concept describes a virtual interchange where through different conversion, distribution, and storage technologies, different energy carriers are linked to the demanded loads. The redundancy of some energy sources or hub technologies allows the energy system problem to be formulated as an optimisation problem, where the objective is to minimise cost variables assigned to these sources or technologies. Example of these cost variables are financial costs, carbon emissions, and availability. Mixed-Integer Linear Programming (MILP) problem is proposed as the optimisation formulation for an energy hub problem.

The energy hub problem formulation is further developed in [40] to include more operational constraints. The study shows that including storage losses, binary control, state change limits, temperature-dependent efficiencies and unit step functions for part-load efficiencies lead to a more accurate plant performance. In [41], the concept is expanded to address the growing need of modelling decentralised energy systems (DES). The study proposes that multiple hubs are modelled and linked to mimic the energy flow behaviour in a neighbourhood. It is also possible to link these hubs into a larger district heating system or other district-level technologies. The Ehub Modelling Tool [42] is subsequently introduced as a software package for DES design problems. Four case studies representing the implementation of energy hub as optimisation planning tool for local energy systems are presented in [43].

Energy hub concept is also implemented in another tool called Sympheny [44]. The tool is a User Interface (UI) implementation of the concept that allows an intuitive way for practitioners to formulate, solve, and visualise a DES problem in one single pipeline. The tool is currently able to handle a 15-to-20 building neighbourhood.

As an energy system design tool, CEA [45] allows the optimisation at city district scale with respect to energy, carbon, and financial aspects. The tool combines data and calculations performed in its demand analysis tool [34] with technology data and performance target definitions to evaluate the energy strategy of a district. The tool introduces five additional modules: resource potential module to generate locally available resources, system technology module to aggregate boundary conditions and performance factors of each technology, system optimisation module to optimise the energy network size, decision module to select configurations that meet the target definitions, and spatio-temporal analysis module to visualise the results in a 4D interface.

A.3 Energy Communities

Multiple studies [46, 47, 48, 49, 50, 51] have been performed to explore the implementation of decentralised energy communities. These recent researches in this frontier show the growing interests and needs in comprehensively studying the benefits and feasibility of an energy community.

In [46], the economic viability of a heat prosumer is assessed through the lens of heat price models. The study proposes the use of water tank thermal energy storage to improve economic performance of a prosumer. Tested at a campus district heating system in Trondheim, Norway, the methodology proves a cost saving of 9% in annual heating and 10 year recovery time for initial investments.

Similar concept using storage technologies has been proposed in [47] for PV prosumers. A cost optimal solution is derived from the mix of batteries, electric vehicles, heat pumps, and thermal heat storage. The study concludes that maximising self consumption of solar energy generated from the PV is the most economical option for the majority of households across the world.

Another study [48] looks at heat and electricity prosumer communities in Finland and the Netherlands from not only economic perspectives, but also from carbon emissions. The study explores five different producing technologies: Ground Source Heat Pumps (GSHP), Air Source Heat Pumps (ASHP), wood pellets boilers, natural gas boilers, and PV. The optimisation is also affected on whether prosumers are able to export their energy production. The study finds that in those two countries, heat pumps represent the optimal technology solution.

A study [49] on transforming residential clusters to electricity prosumers was performed in Sweden. It explores the interconnectedness of electricity vehicle penetrations, storage, and energy networks affect PV sizing and performance indicators. Using three buildings for renovation in Ludivika as case study candidates, the study concludes the feasibility of creating new smart electricity prosumers with high self consumption rates.

Identifying the emerging importance of integrated community energy systems, [50] proposes a performance assessment framework of these systems. Considering localities in the Netherlands, the study shows that a community benefits from cost and emission reductions from providing integrated local energy source alternatives compared to solely relying on the grid. Being fully independent of the grid, however, is found to be still very costly, albeit environmentally beneficial.

Electric vehicle technology is one of the newest players with significant influences in multi-energy districts. The study [51] aims to integrate the flexibility of this energy entity to the design of an energy district. With an appropriate number of vehicles, the technology acting as decentralised energy carriers provides both supply and demand flexibility to the district.

Appendix B

Tool Comparison

In this section, the tools required for this study on economic and environmental assessment on heat prosumer communities are compared and reviewed. There are two main categories of tools needed for such assessment. First, the building demand profiles, which include space heating, domestic hot water, and electricity, are gathered. Second, energy system design tools are utilised to model a decentralised heat network and solve the optimisation problem introduced in it. At the end of this chapter, two appropriate tools from each category are proposed for the methodology of this study.

B.1 Building Energy Demand Tools

To determine the appropriateness of an energy demand tool for this study, the desired characteristics of demand datasets are first evaluated. Building demand evaluation is required in the study as an essential input to the design of an energy system. There are six features in demand datasets regarded to be relevant for conducting such design: the modelling approach used by the demand tool, the spatial resolution of the modelling, the temporal resolution of its analyses, the energy type of output, the location intended for the tools, and the capability of including district influences in the model.

The approach used and the spatial granularity of a demand modelling tool are important to determine the rigour of the results produced. The level of precision in the demand modelling is correlated with that of the system design. In this study, the intended system design resides on the scale of decentralised, small-to-medium neighbourhood. For this scale, a more precise physics-informed model with at least multi- thermal-zone in a building is needed.

The technology mix involved in designing an energy system requires formulations in time-steps. It is critical that the demand dataset temporal resolution is synchronised with functions specified in the system design. In this study, an hourly time-step is chosen for the design.

The types of energy demand outputted from the modelling tools are assessed to address the load balance constraint needed in the system design. The study focuses on three energy demands: space heating, domestic hot water, and electricity. Space cooling is excluded in this study under the assumption that most Swiss houses are yet to be equipped with appropriate technologies for cooling. It is also noted that the consumer end-use demand is required. This category implies the clear separation of the three energy uses. The heating demands include all energy, even electricity through heat pumps, required to rise the intended space or water temperature. End-use electricity demand only consists of other appliances not required for heating.

Local contexts play a significant role in the development of a modelling tool. As most tools require geometrical and geographical inputs, the simulation capability and the outputs are linked with that information. This study centres around decentralised energy systems in Switzerland. Tools that are able to capture such locality are preferred in this study.

Interactions between different buildings are key components in modelling energy demand at district level. Not all tools possess similar capacity to model such interactions. In this study, the consideration of surrounding buildings in the demand calculation for a particular building is important. The demand profiles that explicitly taking into account such factors are better representing the dependencies described in the system design.

Table B.1 summarises all selected tool features for the review analysis. SIA2024 is an adequate tool for estimating most typical buildings in Switzerland. It allows for multiple zones implementations by proportional estimation. The hourly output of all end-use energy consumption can be determined through specified schedules. However, one drawback of using standard values stipulated in a code of practice the values tends to overestimate the actual energy consumption. The types of buildings represented in this method, although extensive, do not cover unique buildings in urban settings.

TRANSYS, CITYSIM, IDA ICE, Umi, and CESAR are the more suitable tool candidates in terms of their modelling approach. The physics-based bottom-up approach suits well for the requirement of this study. They also satisfy the required spatial and temporal resolutions. Three other features differentiate these five tools. TRNSYS and CESAR are the two tools that provide complete demand profiles needed for this study. While for locality, Swiss contexts are captured in CITYSIM, IDA ICE, and CESAR. Most tools except for TRNSYS are capable of demand modelling taking into account district analysis explicitly.

Buildings in CEA are simulated in considerations of their physical attributes and behaviour. To meet the tool objective of designing larger city scale and maintain tractability, CEA utilises statistical methods to projects its physics-based demand forecasting for annual results. The tool takes a hybrid modelling approach that is still appropriate for this study. In terms of spatial resolution, however, CEA simplifies a building into a single zone, disregarding vertical separations of each storey. The database and contexts developed are specifically tailored for two cities: Zurich and Singapore.

Top-down methods selected in this review are end-use and spatio-temporal methods. These tools are intended to decompose aggregated demand data of a city and create energy use density forecasts. While they are useful tools for larger scale planning, such tools do not provide the required spatial resolution of a single-building energy demand profile in this study.

Table B.1: Features of selected energy demand tools

Demand Modelling Tools	Modelling Approach	Spatial Resolution	Temporal Resolution	Energy Output	Locality	District Analysis	References
SIA2024	standards	multi-zone per floor	hourly	Elec., SH, SC, DHW	Switzerland	none	[24]
TRNSYS	bottom-up	multi-zone per floor	hourly	Elec., SH, SC, DHW	USA, France, Germany	none	[26][27]
CITYSIM	bottom-up	multi-zone per building	hourly	SH, SC	Switzerland	explicit	[28]
IDA ICE	bottom-up	single-zone per floor	hourly	SH, DHW	Sweden, Switzerland, Germany, Finland	explicit	[29][32]
Umi	bottom-up	single-zone per floor	hourly	Elec., Gas	USA	explicit	[30][33]
CESAR	bottom-up	single-zone per floor	hourly	Elec., SH, SC, DHW	Switzerland	explicit	[31][33]
CEA	hybrid	single-zone per building	hourly	Elec., SH, SC, DHW	Zurich, Singapore	explicit	[34]
End-use method	top-down	single-zone per city block	annual	Elec., SH, SC, DHW	New York City	implicit	[35]
Spatiotemporal method	top-down	single-zone of 100m block	hourly	Elec., SH, SC, DHW	Helsinki, Shanghai	implicit	[36]

Aside from demand modelling tools, energy profile of a building is measurable. This approach is one alternative to using modelling tools altogether. The advantages of direct measurement are that it is generally precise in detecting actual use profiles, and it captures deviations in similar use building. However, it is noted that direct measurement often involves smart grids and sophisticated meters. This condition presents a bias in the measured datasets to capture more state-of-the-art or modern buildings. This study, although acknowledges the possible contribution of direct measurement datasets in this topic, is not considering this approach.

B.2 Energy System Design Tools

The energy system design tools are reviewed based on the final objective of this study. The features, deemed important for the tools to have, are multi-energy carrier definitions, the energy technology mixes available, multi-building formulation, multi-objective optimisation, and the metrics used for evaluation.

Three tools are evaluated in this study: Ehub, Sympheny, and CEA. Table B.2 summarises the comparison of these tools. Most energy system design tools have included features that are necessary for this project. They generally are equipped with multi-building problem formulations, multi-objective optimisation, and the ability to evaluate the technology mixes in terms of economic and environmental metrics. CEA is notable short in terms of the ability to simulate multi-energy carriers in a single building. Storage technologies are also not yet considered in CEA. As Sympheny is a UI implementation of Ehub, Sympheny shares most functionality with it.

Table B.2: Features of selected system design tools

System Design Tools	Multi-Energy Carriers	Transformation Technologies	Conversion Technologies	Storage Technologies	Distribution Technologies	Multi-Building Formulation	Multi-Objective Optimisation	Economic Evaluation	Environmental Evaluation	Modelling Flexibility	References
Ehub	✓	✓	✓	✓	✓	✓	✓	✓	✓	High	[39][40][41] [42][43]
Sympheny	✓	✓	✓	✓	✓	✓	✓	✓	✓	Medium	[44]
CEA	✗	✓	✓	✗	✓	✓	✓	✓	✓	Medium	[45]

One deciding factor taken into account in this review is how flexible the modelling tools are. Flexibility here is defined as how much freedom users can develop and define their own technologies and networks. Sympheny and CEA are tools developed with practical user centred design. While they are more intuitive to be used by practitioners, modelling for new studies can be limited. Sympheny, for example, requires users to geographically identify the modelled buildings within a predefined

GIS dataset. CEA also limits the technologies to several predefined categories. As this study is trying to formulate a novel framework in assessing the economic and environmental impacts of heat prosumer communities, a higher degree of flexibility is required. This flexibility is provided in Ehub through its extensive programmable modules.

B.3 Selected Study Tools

Through the reviews, CESAR is regarded as the most suitable for building energy modelling tool in this study. It has the suitable precision in its simulation and outputting all the required demand profile with Swiss local context. For the energy system design, Ehub is selected as the appropriate tool for a novel formulation. Its flexible and extensive features allow the implementation of the framework proposed in this study.

Appendix C

Building Heat Capacity

Building Heat Capacity Calculation

Based on ISO52016

Input Data

Building size

L(m)	10
W(m)	7
Floors	2
H(m)	3
Int_walls_per_ext	1

A_heated(m2)	140
A_footprint (m2)	70
A_extwalls(m2)	204
A_intwalls(m2)	204

Spec. heat opaque elements

Table B-14

Calc. Class	Areal Specific Heat (J/m2K)	ISO Class	Remarks
A	50000	Very Light	No massive components
B	75000	Light	5-10 cm lightweight brick/concrete
C	110000	Medium	10-20 cm lightweight brick/concrete or <7 cm heavy brick/concrete
D	175000	Heavy	7-12 cm heavy brick/concrete
E	250000	Very Heavy	>12cm heavy brick/concrete

Spec heat internal (J/m2K)

Table B-17

Calc. Class	Areal Specific Heat (J/m2K)	ISO Class	Remarks
Int	10000	-	-

Heat Capacity Calculation:

Spec heat	Ref area (m2)	Class	Areal specific heat (MJ/m2K)	Specific heat (MJ/K)
Internal air/furniture	140	Int	0.01	1
Internal floors	70	A	0.05	4
Internal walls	204	A	0.05	10
External walls	204	C	0.11	22
Roof	70	C	0.11	8
External floors	70	C	0.11	8

Building Heat Capacity = **53** MJ/K

= **15** kWh/K